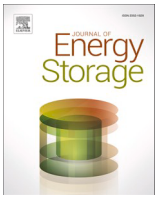
Journal of Energy Storage 183 (2027) 125667



Contents lists available at ScienceDirect

Journal of Energy Storage

journal homepage: www.elsevier.com/locate/est



Review Article

A comprehensive review of the numerical and experimental developments of close-contact melting for phase change material applications

Daut Mustafic [a], Fatma Al-widyan [a], Nick S. Bennett [a], Mohammad S. Islam [a,*]

[a] School of Electrical, Mechanical and Biomedical Engineering, University of Technology Sydney, Ultimo, NSW, 2007, Australia

ARTICLE INFO

Keywords:
CCM
PCM
Energy storage
Thermal management
Modelling
Experiment

ABSTRACT

Close-contact melting (CCM) offers a route to improving heat-transfer rates while exploiting the high latent energy density of phase change materials (PCMs) for thermal management and energy storage. However, the modelling and experimental developments needed for practical adoption remain fragmented. This review synthesises numerical and experimental CCM research to identify the capabilities and limitations of existing methods and the next steps towards application. It compares computational frameworks for coupling melt flow, heat transfer, phase change and solid-body motion, including implementations within established CFD and multi-physics software. Recent pressure-corrected momentum-source models are also examined, including their extension to piston-driven melting in cylindrical capsules. Experimental pressure-enhanced CCM configurations are highlighted as a promising route to higher power density, with a maximum reported enhancement of approximately fourfold relative to gravity-driven operation under specific experimental conditions. Finally, the review outlines application-specific development priorities for thermal energy storage, electronics cooling and battery thermal management, with particular attention to model validation, melt redistribution and repeatable operation. The synthesis is intended to help academic researchers and industrial developers identify the current capabilities of CCM and the steps needed for its practical implementation.

1. Introduction

As energy systems transition towards decarbonisation and electrification, efficient thermal energy storage (TES) and reliable thermal management address two related but distinct needs. TES supports renewable energy use by storing thermal energy when it is available and releasing it when required [1], as illustrated in Fig. 1. Thermal management limits local temperature rises in electronic and power semiconductor devices [2]. Latent heat storage using phase change materials (PCMs) offers substantial energy storage over a narrow temperature range, with applications spanning large-scale TES [3], compact thermal management [4], power electronics [5], batteries [6] and concentrated solar power [7].

The low thermal conductivity of many PCMs limits the rate of heat absorption and release, reducing charging and discharging performance [8]. Conventional enhancement strategies include metallic fins [9], graphite matrices [10], high-conductivity nanoparticles and porous metal foams [11]. These approaches improve heat transfer within the PCM, but may also increase system mass, cost and design complexity. Moreover, a growing liquid layer between the heat source and the remaining solid can introduce additional thermal resistance during melting.

Close-contact melting (CCM) addresses this limitation by maintaining a thin liquid film between the heated surface and the solid PCM, thereby shortening the conductive heat-transfer path [12]. The mechanism has been examined in idealised plate and capsule configurations [13], as well as on engineered surfaces [14]. In gravity-driven CCM, the net gravitational load brings the solid towards the heat source; in pressure-enhanced CCM, an additional applied load promotes contact and melt displacement [15]. These loading modes provide routes to enhancing melting performance without relying solely on increased material conductivity.

Hu et al. (2022) [16] reviewed CCM fundamentals, enhancement strategies and applications for rapid-charging TES. Building on that foundation, this review focuses on the numerical and experimental developments needed to translate CCM into PCM-based TES and thermal management devices. Its distinct emphasis is a solver-by-solver comparison of solid-motion treatments in custom codes, ANSYS Fluent,

* Corresponding author.
E-mail address: mohammadsaidul.islam@uts.edu.au (M.S. Islam).

https://doi.org/10.1016/j.est.2026.125667
Received 28 May 2026; Received in revised form 17 October 2026; Accepted 10 November 2026
Available online 16 November 2026
2352-152X/© 2026 The Authors. Published by Elsevier Ltd. This is an open access article under the CC BY license (http://creativecommons.org/licenses/by/4.0/).

OpenFOAM and COMSOL, including post-2022 developments, with explicit assessment of assumptions, validation and practical method-selection criteria (Tables 4–6). Experimental studies are synthesised by geometry, material, heating conditions and reported performance, with particular attention to gravity-driven and pressure-enhanced configurations. The resulting perspective identifies priorities for coupled CFD–multiphysics modelling and application-specific prototyping, intended to guide both academic research and industrial development. This is a narrative review. Targeted Google Scholar searches use the terms 'close-contact melting', 'contact melting', 'unconstrained melting', 'unfixed melting', 'direct melting' and 'direct contact melting'. The discussion spans foundational work through studies published in 2026; papers are selected for their relevance to the physical scope in Section 2.1.

2. Background and early work

2.1. Terms and definitions

CCM is considered here in the context of PCM-based energy storage and thermal management. Its defining feature is a thin melt film maintained between the solid PCM and a heated surface as the solid and heat source approach one another. Table 1 distinguishes terms describing this mechanism, the freedom of the solid to move, the moving component and the source of the applied load [13,16]. These categories are related but are not interchangeable.

In particular, unconstrained or unfixed melting describes the freedom of the solid to move, whereas CCM describes the heat-transfer mechanism at a close-contact region. PCM-driven and heat-source-driven refer to which component moves; gravity-driven and pressure-enhanced refer to the loading mechanism. Internal and external CCM

Table 1
Terminology used in CCM research and the distinctions adopted in this review.

Term	Definition / usage	Key distinction
Close-contact melting (CCM)	Melting through a thin liquid film between a heated surface and an approaching solid [13,16].	Describes the heat-transfer mechanism; the solid is separated from the heater by melt.
Contact melting	Melting through a thin liquid film between a heated surface and an approaching solid [13,16].	Used as CCM here when the close-contact configuration is specified.
Direct melting / direct contact melting	Terminology emphasising melting adjacent to a heated contact surface [17].	Not treated as a separate physical mechanism in this review.
Unconstrained / unfixed melting	Melting in which the remaining solid is free to move within its surroundings [18,19].	A mobility condition; CCM and bulk convective melting may coexist.
PCM-driven CCM	The PCM solid moves towards the heat source [16].	Classifies the moving component; see Fig. 2(a).
Heat-source-driven CCM	The heated body moves into the PCM [16,20].	Classifies the moving component; see Fig. 2(b).
Gravity-driven CCM	The net gravitational load drives the solid towards the heated surface [16].	Classifies the load; performance depends on orientation and density difference, see Fig. 2(a).
Pressure-enhanced CCM	An additional applied load promotes close contact and melt displacement [15].	Classifies the load; includes piston- or weight-loaded configurations; Fig. 2(c)
Dynamic PCM (dynPCM)	Term used for the pressure-enhanced PCM concept reported by Fu et al. [15].	Retained for literature identification; pressure-enhanced CCM is used elsewhere; Fig. 2(c)

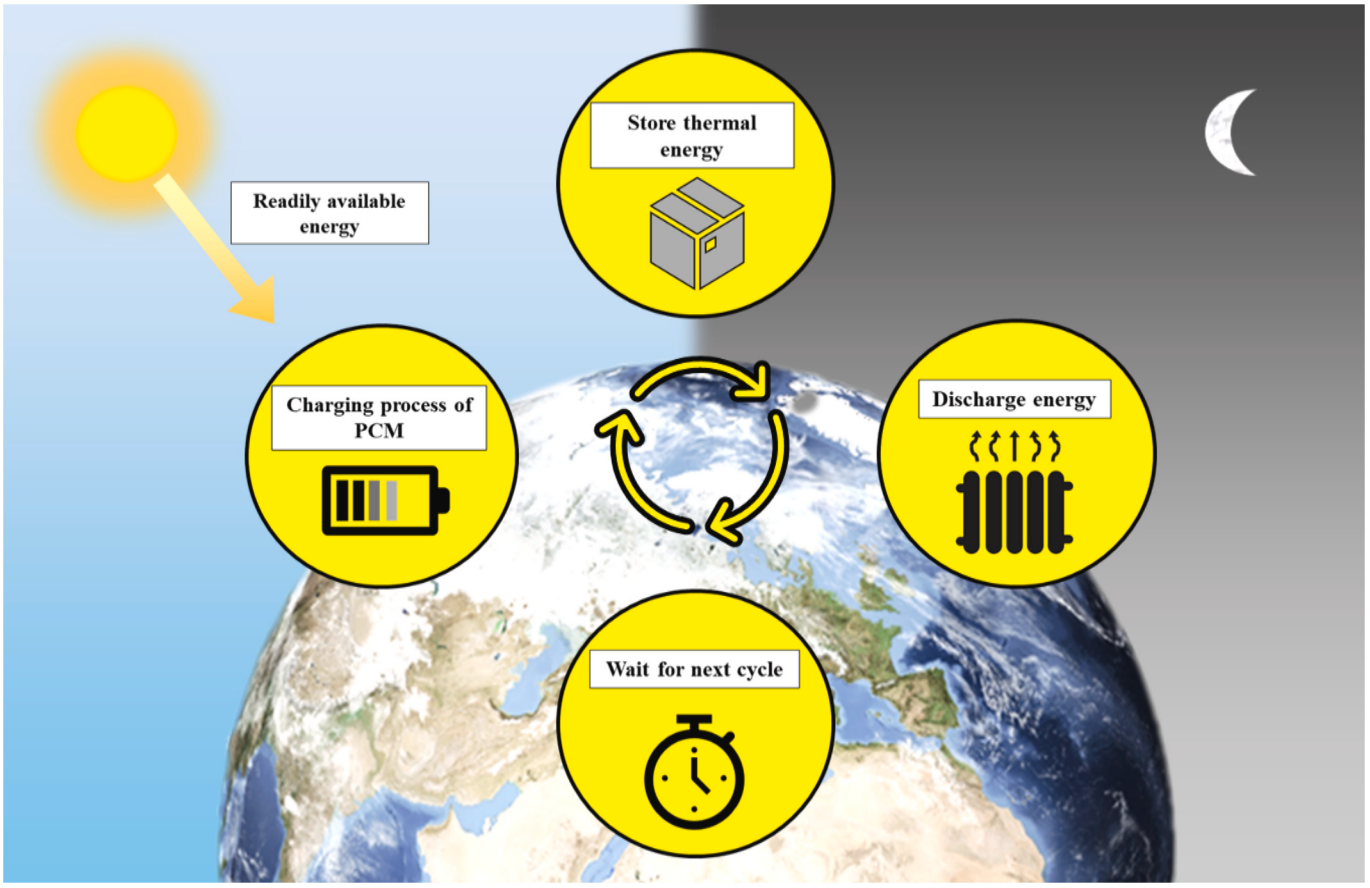


Fig. 1. Using PCMs for renewable thermal energy storage in domestic and industrial heating and cooling applications.

are additional labels used in particular formulations [20,21] and should be interpreted with reference to the geometry and reference frame of the cited study.

In PCM-driven CCM, the solid moves towards the heated surface, commonly under its net gravitational load, as shown in Fig. 2(a). In heat-source-driven CCM, the heated body moves into the PCM, as shown in Fig. 2(b). Both require a route for the melt to escape or be redistributed. The heat-source-driven mode remains relatively unexplored within PCM-based TES and thermal management; the examples discussed here include thermal drilling and moving thermal probes. The main emphasis of this review is therefore PCM-driven CCM.

Pressure-enhanced CCM applies an additional mechanical load, for

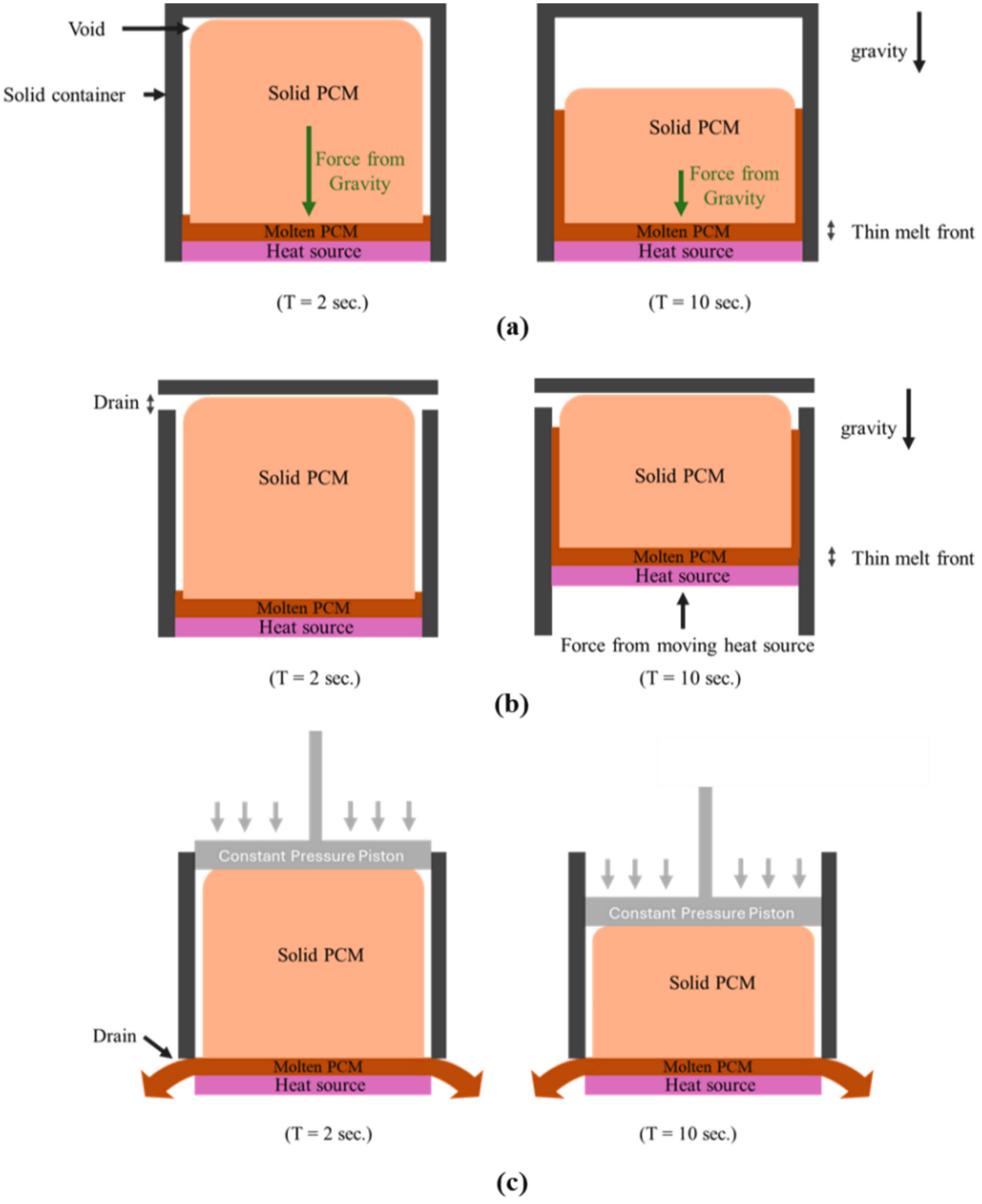


Fig. 2. CCM configurations: (a) PCM-driven and (b) heat-source-driven melting, and the addition of an actuating system to provide (c) pressure-enhanced CCM (dynPCM) for the PCM-driven mode.

example through a piston, to maintain close contact, as shown in Fig. 2 (c). The term dynamic PCM (dynPCM) is retained in Table 1 to connect with the terminology used by Fu et al. [15]; elsewhere in this review, pressure-enhanced CCM is used consistently. Unlike gravity-only loading, externally applied loading can be directed towards the heated surface independently of the device orientation, provided that melt redistribution is accommodated.

The primary mode of heat transfer in CCM across the melt interface is thermal conduction [22]. Although natural convection can develop within the melt layer, in particular with geometries where horizontal surfaces are combined with vertical temperature gradients, its effect is usually limited in CCM [23]. This is because the melt film remains extremely thin, typically on the order of 0.1–1 mm [24], which constrains the development of buoyancy-driven flow. As a result, convection currents are either negligible or contribute only marginally to the total heat transfer. Studies and scaling analyses suggest that convection accounts for no more than ~10–15% of the overall heat transport in most low-Stefan-number capsule cases [25], and is not a general upper limit for practical CCM systems. Convection currents and Rayleigh–Bénard cells are observed in latent heat storage systems [26]; however, such flows are typically suppressed within the thin close-contact melt film.

For TES and thermal management, volumetric energy density, E_v, is defined here as the increase in thermal energy of a specified system relative to its initial state, divided by a fixed reference volume, V. With $Q(t)$ denoting the net thermal energy stored, including sensible and latent contributions,

$$E_v(t) = \frac{Q(t)}{V} \tag{1}$$

Storage power density is the time derivative of energy density:

$$P_v(t) = \frac{dE_v}{dt} = \frac{1}{V}\frac{dQ}{dt} \tag{2}$$

E_v and P_v have units of J m^{-3} and W m^{-3}, respectively. Constant net power retained by the system produces a linear rise in E_v.

2.2. Background to analytical formulation

The study of phase change processes, particularly melting and solidification, has long relied on the Stefan problem as a foundational model [27]. Originally formulated to describe the freezing and melting of ice in the Arctic in the year 1890, the Stefan problem captures the transient movement of an interface between solid and liquid phases under heat conduction. This model is foundational for understanding the fundamental physics of phase change before introducing more complex mechanisms such as convection, dynamic boundary conditions, pressure effects, etc.

In its classical form, the one-dimensional Stefan problem assumes a semi-infinite domain subject only to thermal conduction. The material is initially at a uniform temperature, and melting is induced by imposing a boundary temperature higher than the melting temperature at one end. No internal heat generation is considered, and the effects of fluid motion, volume change, or pressure gradients are neglected. As a result, the governing physics are reduced to a one-dimensional transient heat conduction equation, i.e. a diffusion problem,

$$\frac{\partial T}{\partial t} = \alpha \frac{\partial^2 T}{\partial x^2}, \tag{3}$$

where $T(x,t)$ is the temperature field (either in the liquid or solid region), t is time, x is the spatial coordinate, α is the thermal diffusivity of the material.

This governs the solid and liquid regions separately. The moving interface or boundary position where melting or solidifying is occurring is defined as $x^*(t)$, and exists between the solid and liquid regions. The temperature at the interface remains constant and equal to the material's melting temperature, T_m, due to phase equilibrium. The interface movement is determined by the conservation of energy applied at the boundary. The rate at which the phase change occurs must be equal to the net heat flux entering the interface defined by Fourier's Law of Heat Conduction balanced with the latent heat of the material. This expression provides us the Stefan condition,

$$k_s \left.\frac{\partial T_s}{\partial x}\right|_{x^*} - k_l \left.\frac{\partial T_l}{\partial x}\right|_{x^*} = \rho L \frac{dx^*}{dt}, \tag{4}$$

Even considering the simplifications stated here, obtaining exact analytical solutions remains difficult or impossible. Obtaining transient solutions to the governing partial differential equations (PDEs) is not trivial, and so similarity solutions may be implemented. These similarity variables transform the equation into an Ordinary Differential Equation (ODE) using error functions. The same process is applied to the moving interface in eq. (4), using similarity variables to characterise the position of the moving interface over time.

The theoretical framework for analysing CCM within PCM systems is fundamentally rooted in the classical Stefan problem, which defines heat transfer-driven phase transitions with a dynamic boundary. Early modelling efforts employed simplified assumptions, such as steady-state heat transfer, conduction-only and planar configurations to obtain tractable solutions. Over the years, more accurate details were incorporated into these models, including temperature-dependent properties, convection modelling, and non-isothermal conditions. Many approaches require iteration in the form of semi-analytical or semi-numerical methods, instead of a purely analytical solution. These models utilised advanced techniques like perturbative methods, integral transformations, or numerical inversion to address the complexities of nonlinear behaviour and moving boundaries. Despite these analytical advancements, obtaining exact analytical solutions remains difficult. Table 2 shows early works which employ these methods to model CCM.

A key characteristic of this field is its reliance on idealised configurations and boundary conditions. The resulting equations are typically tailored to specific setups, such as flat surfaces in contact with rectangular PCM blocks or spherical enclosures experiencing radial melting, which limits their applicability to broader scenarios. This scenario-specific nature reduces the generalisability of such models, making them less suitable for complex real-world implementations involving irregular shapes or time-dependent conditions.

Additionally, experimental validation presents significant challenges due to the difficulty in observing and quantifying thin melt films, interfacial heat transfer rates, and dynamic melting fronts with sufficient

Table 2
Early analytical modelling of gravity-driven CCM.

No.	Ref.	Year	Geometry	Key contributions
1	[28]	1986	Moving heat source - 2D axisymmetric cylinder	Heat source velocity
2	[29]	1986	Rectangular solid blocks (2D Cartesian) + Circular cylindrical solid blocks (2D axisymmetric)	Solid height melting velocity
3	[30]	1997	Spherical Capsule	Governing equations with Convection in liquid
4	[31]	1997	Cylindrical and Spherical Capsule	Cylindrical Capsule Melting Velocity Spherical Capsule Melting Velocity
5	[21]	1999	Axis symmetric (Spherical, cylindrical, rectangular)	Generalised Melting Rate Equation
6	[32]	2000	3D Rectangular Flat Plate	Force Balance Equation
7	[33]	2001	2D Rectangular	Normalised Force Balance Equation Mean Normalised Nusselt Number

precision. A large group of studies have focused on analysing and experimentally validating their analytical correlations for cylindrical geometries, summarised in Table 3.

Consequently, while theoretical models provide essential insights and scaling analyses, their practical application often necessitates computational or experimental methodologies to overcome existing limitations.

3. Developments of numerical models

3.1. Background to numerical approaches

Numerical modelling of melting and solidification is widely used to investigate thermal behaviour, support system design and complement experiments. The governing conservation equations are discretised over a computational mesh. ANSYS Fluent and OpenFOAM employ the finite volume method (FVM), which expresses conservation over each control volume; COMSOL Multiphysics commonly uses the finite element method (FEM). Spatial discretisation is distinct from the treatment of phase change and from the method used to identify material interfaces. Fig. 3 summarises these categories of modelling choices.

When the PCM shares a domain with an immiscible fluid such as air, the volume of fluid (VOF) method can be used to capture the material interface. Its volume fraction distinguishes PCM from air, whereas a separate liquid fraction, β, identifies the solid and liquid states within the PCM. These variables serve different purposes: VOF captures the free surface, while the liquid fraction links phase change to the energy and momentum equations. This distinction is explicit in the recent model by Sahray et al. [39]. A separate VOF model is not required merely because PCM melts or because a heat-transfer fluid is modelled in a neighbouring, wall-separated domain; the latter can instead be treated through conjugate heat transfer.

Among the numerical methods, *fixed-grid approaches* are the most widely adopted, particularly in general-purpose CFD software. These methods avoid explicitly tracking the moving solid–liquid interface and instead rely on unified formulations over the computational domain. They solve a single set of conservation equations (mass, momentum, energy) for both phases, with appropriate modifications to account for phase change, such as latent heat and velocity suppression to mimic rigid, solid regions. This makes fixed-grid methods popular for multi-dimensional and complex geometries where adaptive or moving mesh techniques become computationally intensive or unstable.

The incompressible continuity equation (mass equation) is expressed as

$$\nabla\cdot\mathbf{u} = 0, \tag{5}$$

where u is the velocity vector. The conservation of momentum is written as

$$\frac{\partial(\rho\mathbf{u})}{\partial t} + \nabla\cdot(\rho\mathbf{u}\mathbf{u}) = -\nabla p + \mu\nabla^2\mathbf{u} + S, \tag{6}$$

where ρ is the local density, μ is dynamic viscosity, and S represents either a source term (such as gravity in the vertical component) or a sink term. The enthalpy-based energy equation is expressed as

$$\frac{\partial(\rho h)}{\partial t} + \nabla\cdot(\rho\mathbf{u}h) = \nabla\cdot(k\nabla T), \tag{7}$$

where h is the specific enthalpy *and* k is the thermal conductivity.

Within the fixed-grid framework, several energy equation reformulations have been developed to handle the latent heat effect. These include the *enthalpy method, apparent heat capacity method, effective heat capacity method,* and *source-based enthalpy method* [40]. In the enthalpy method, latent heat is incorporated directly into the total enthalpy term on the left-hand side (LHS) of the energy equation, allowing the temperature–enthalpy relationship to govern the evolution of the phase front. The apparent heat capacity method modifies the specific heat over a phase change interval to account for latent heat, making it easier to implement in certain solvers. The effective heat capacity method, a simplification of the previous, integrates the apparent heat capacity over the melt range to use a constant "effective" value, often at the expense of accuracy. In contrast, the source-based enthalpy method places the latent heat term on the right-hand side (RHS) as a source or sink, based on the local change in liquid fraction. Each method has trade-offs. While the apparent heat capacity method generally offers greater stability due to enhanced diagonal dominance in the discretised equations, the source-based methods provide finer control over latent heat release but may suffer from slower convergence or instability near steep phase transitions.

A phase-state marker expressed as the liquid fraction, β, is then introduced to indicate the extent to which each computational cell is solid or liquid. This variable provides the link between the temperature field and the latent heat treatment, since the local phase state determines how much latent energy has been absorbed or released. In the absence of phase change, and for specified velocity and constant properties, the discretised energy equation is comparatively straightforward and behaves as a linear diffusion–convection problem. Once latent heat is introduced, the energy equation becomes strongly coupled to the unknown liquid fraction field, making the problem nonlinear and often difficult to converge, particularly near the melting front where small temperature changes can produce large changes in phase fraction.

To address this, CFD solvers such as ANSYS Fluent use iterative procedures based on the formulation of Voller and Swaminathan [41], in which the temperature field and liquid fraction are repeatedly updated until they become mutually consistent.

3.2. Key limitations in numerical approaches for CCM – velocity damping

A central challenge in conventional fixed-grid PCM modelling is that fluid momentum equations do not, by themselves, impose rigid-body translation or rotation. The limitation considered here is the stationary-solid momentum closure used with standard enthalpy–porosity implementations, rather than the enthalpy representation of latent heat. In conventional PCM melting simulations, solid regions are usually treated as either static zones or zones with severely damped motion. This is primarily achieved by suppressing the velocity field in regions with high solid fraction (typically where the melt fraction approaches zero).

Three common treatments are distinguished. The fixed-velocity

Table 3
Recent validated models on cylindrical geometries, including annular and finned variants.

No.	Ref.	Year	Considers pressure-enhanced CCM	Key contributions
1	[34]	2014	☐	Analytical Melt Fraction Expression for Finned Geometry
2	[15]	2022	☒	Melt-Front Position Equation Thermal Resistance Equation Predictive Model for Performance
3	[35]	2024	☒	Peak Heat Flux Power Requirement Equation for generating applied pressure: Figures of merit: Peak heat flux potential and Efficiency, heat flux to power flux ratio
4	[36]	2024	☐	Dimensionless correlation for the mushy zone constant (Am) Practical equation for calculating Am
5	[37]	2024	☒	Thermal Convection Model
6	[38]	2024	☒	Plateau Temperature Scaling Heat Flux Distribution Equation Thermal Conductance

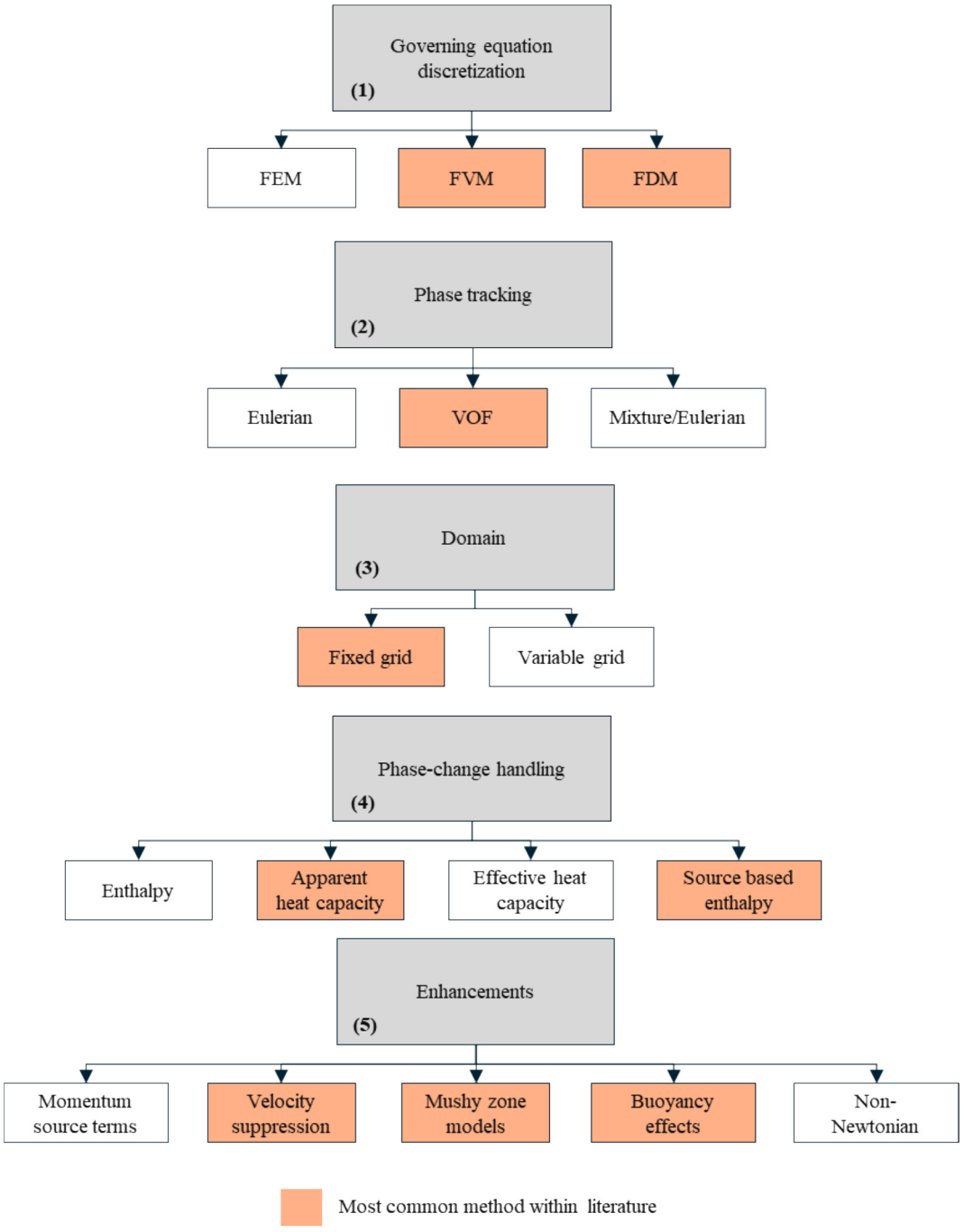


Fig. 3. Different approaches to numerical modelling of PCM melting in CCM context.

method sets the velocity of solid cells or faces to a prescribed value, usually zero, through constraints in the discretised momentum equations [42]. In its stationary form, this is appropriate when solid motion is absent, but it cannot represent the descent or rotation of a freely moving solid. The increased-viscosity method instead assigns a large effective viscosity as the solid fraction increases [43]. This resists local deformation; it does not necessarily eliminate bulk translation of the high-viscosity region.

The increased-viscosity approach should therefore not be dismissed categorically. Kasibhatla et al. [43] reproduced melting and settling in an encapsulated PCM using a variable-viscosity formulation and assessed the influence of the assigned solid viscosity and pressure–velocity convergence. Nevertheless, the large viscosity contrast can make the discrete momentum problem stiff and convergence demanding. This limitation arises through the viscous stress treatment. A converged temperature field or total melt fraction alone does not demonstrate that the solid velocity and shape are accurately reproduced.

For engineering assessment, variable viscosity is most defensible when aggregate quantities such as melt fraction or charging time are the primary outputs, and any artificial deformation has a demonstrably small effect on those outputs. Its viscosity law, limiting value and convergence settings must be checked for the material properties and operating conditions under consideration. It is less suitable as a predictive model when exact rigid-body shape, rotation, clearances or wall contact control the melt-film dynamics, because high viscosity alone does not impose an exact rigidity constraint. The practical choice is therefore between a calibrated approximation and an explicitly constrained solid-motion model, rather than between an inherently

unstable and an inherently stable method.

The Darcy-source method represents the partially solidified region as a porous medium and introduces a resistance that increases as the liquid fraction decreases [44]. Its usual stationary-solid form damps velocity towards zero. An extended form can instead penalise velocity relative to a separately calculated solid-body velocity, as in the settling approaches discussed in Section 3.3. This is distinct from merely reducing the mushy-zone constant to permit movement. Separately, inappropriate mushy-zone constants, inadequate melt-film resolution or incomplete convergence can distort the predicted flow and melting rate. Parameter, mesh and time-step sensitivity must therefore be assessed independently of whether the formulation includes a consistent solid-motion model; tuning alone does not supply a rigid-body constraint.

These treatments are useful within their intended assumptions, but their ability to reproduce CCM must be assessed against the required solid motion and interface geometry. Stationary velocity fixing cannot capture a moving solid; viscosity and empirically tuned Darcy treatments can approximate motion without guaranteeing rigidity. Where solid translation or rotation governs heat transfer, the selected formulation must couple phase change, melt flow and solid dynamics consistently, and be validated beyond a single fitted melting-time curve.

3.3. Recent numerical models of CCM

Numerical modelling of CCM with PCMs follows two broad implementation routes: models developed within established commercial platforms, such as ANSYS Fluent and COMSOL Multiphysics, and custom-built codes tailored to particular geometries and assumptions. While these commercial software tools offer user-friendly interfaces and robust solution capabilities, only a limited number of studies have successfully simulated the entire CCM process within these environments. These simulations often encounter challenges in accurately modelling solid body motion, melt film dynamics, and phase interface behaviour without resorting to significant simplifications, such as fixed geometries or empirically derived mushy zone constants.

Consequently, most high-fidelity simulations rely on in-house developed codes that incorporate advanced features like rigid-body dynamics, adaptive mesh refinement, and Lagrangian or VOF-based interface tracking methods. However, these custom-built codes are rarely made publicly available, which leads to limitations in terms of reproducibility, peer validation, and broader community adoption.

Custom-built solvers are considered first to explore how authors directly customise and modify individual parameters that may be locked away or inconvenient to access in commercial software. A synthesis of in-house solvers is presented in Table 4, highlighting reported accuracy, experimental validation, and the geometry considered. In Tables 4 and 5, qualitative agreement and calibration descriptions are distinguished from numerical error measures. “Not quantified” means that no numerical error measure is tabulated here; these descriptions guide interpretation rather than provide a common accuracy ranking.

A key step seen throughout many of the following studies is evaluating the force balance on the solid region of the material to be able to determine the predicted sinking velocity. Fig. 4 illustrates the forces acting on the solid, namely the pressure, gravity, viscous, and inertial forces. The ‘buoyancy’ or ‘liquid film pressure’ is the most difficult to capture due to the complicated physics occurring such as volume expansion, convection effects, and thin film dynamics. Certain studies choose to not evaluate the forces directly throughout the transient process, and instead impose the thin melt film conditions derived from thin film lubrication theory [58,59].

Hong and Saito [17] developed one of the earliest methods to model transient and non-quasi-static behaviour of solid motion using the

Table 4
Gravity-driven CCM models using custom-built solvers.

No. #.	Ref.	Year	Experimental validation	Shape / geometry	Accuracy / agreement	Key contribution
1	[17]	1993	☐	2D rectangular block	*Not quantified*	The liquid layer remains thin and heat conduction dominates at low Stefan numbers, but convection effects become significant at higher Stefan numbers, causing discrepancies with analytical solutions.
2	[34]	2014	☒	2D axisymmetric vertical annular enclosure	Qualitative agreement, especially at early times	The combined enthalpy and CCM model predicts: Melt fraction, thin melt film thickness (~0.5 mm), heat transfer rate.
3	[23]	2015	☒	2D Radial coord. Horizontal cylindrical shell	<10% deviation at later times	CCM increases melting rate by up to 2.5× in lower parts of the system, compared to regular convective melting.
4	[20]	2017	☐	(1) 2D planar (rectangular) (2) Axisymmetric cylindrical	Not quantified	Quasi-steady, Lagrangian modelling of close-contact melting is possible with high expected accuracy and low computational cost.
5	[45]	2017	☒	2D Rectangle	Not quantified	The new enthalpy-based approach accounts for solid bulk motion without parameters like the mushy zone constant, which often lead to unrealistic deformations in traditional methods.
6	[46]	2021	☒	3D Vertical Cylinder (axisymmetric)	Qualitative agreement	The model successfully captures combined CCM and convective melting, including: thin melt film dynamics, solid PCM sinking, transition from conduction- to convection-dominated melting.
7	[47]	2022	☐	2D cylindrical coordinates	Not quantified	CCM on superhydrophobic surfaces is generally worse than on regular (no-slip) surfaces, primarily due to thermal slip, despite the presence of hydrodynamic slip.
8	[48]	2023	☒	3D Vertical Cylinder (axisymmetric)	5% mean error in melt fraction for the first 60%, up to 25% deviation in later stages	Combined CCM and convection improves performance: doubling the average melting rate compared to convection only despite only a 25% increase in heat transfer area.
9	[49]	2023	☐	2D planar (Moving Heat Source)	Calibrated agreement (qualitative)	Simulation captures: (a) Melting velocity ramp-up behaviour (b) Heat flux and temperature field evolution (c) Movement of the melting probe or tool
10	[50]	2024	☒	3D Vertical Cylinder	7% of molten layer thickness	Yield stress and shear-thinning/thickening effects significantly impact the melting process and that Newtonian models cannot accurately predict.
11	[51]	2024	☒	2D horizontal double-pipe concentric storage unit with longitudinal fins	error in melt fraction is 10%	Model incorporating rigid body motion and the VOF method was developed, successfully predicting the solid phase motion and melting sequences.

Table 5
Recent numerical modelling of gravity-driven CCM using established CFD software platforms.

No. #	Ref.	Year	Experimental validation	Shape / geometry	Accuracy / agreement	Key contribution
1	[18]	2018	☒	3D Vertical Cylinder (axisymmetric)	Calibrated agreement (qualitative)	ANSYS Fluent: The enthalpy-porosity model in Fluent can match experimental melting times if the mushy zone constant is tuned based on the driving temperature difference.
2	[52]	2018	☒	2D Rectangular	Less than 8% of total melting time	OpenFOAM: Implicit force-balance iteration determines a common settling velocity, imposed by an extended Darcy term. A liquid-fraction threshold defines the immersed force-integration boundary; the energy equation retains latent-heat advection.
3	[53]	2024	☒	2D axis-symmetric vertical shell and tube LHTS	Agreement after calibration (qualitative)	ANSYS Fluent: No universal mushy constant exists; it must be tuned per case, making the method impractical for general CCM simulations.
4	[54]	2024	☒	2D axis-symmetric finned latent heat storage	7% deviation in complete melting time	COMSOL Multiphysics: Comparison between CM and CCM: CM is better with upward HTF flow, while CCM performs better with downward flow.
5	[55]	2024	☒	3D Vertical Cylinder	10.88% of liquid fraction evolution	ANSYS Fluent: The Bingham fluid assumption successfully captures rigid solid motion, preventing unrealistic deformation of the solid PCM, which was a limitation in enthalpy-porosity models.
6	[56]	2024	☐	2D & 3D of triplex tube heat exchanger, with longitudinal plate fins	*Poor agreement (qualitative)*	ANSYS Fluent: The enthalpy-porosity method is inadequate for accurately modelling close-contact melting. A low mushy zone constant (10^5) allows solid bulk motion but leads to unrealistic deformation of the solid.
7	[57]	2025	☒	2D Vertical and horizontal rectangles	8.9% of the total PCM height & 9.4% in complete melting time	COMSOL Multiphysics: Aspect ratio affects CCM's enhancement: The closer the aspect ratio is to 1, the greater the improvement in melting rate and thermal homogeneity.
8	[39]	2026	☒	2D axisymmetric cylinder on an open heated plate	Melting-rate and shape agreement	ANSYS Fluent: high mushy-zone resistance with a dynamically pressure-corrected axial source enables coherent descent; PCM–air interface captured by coupled level-set/VOF.

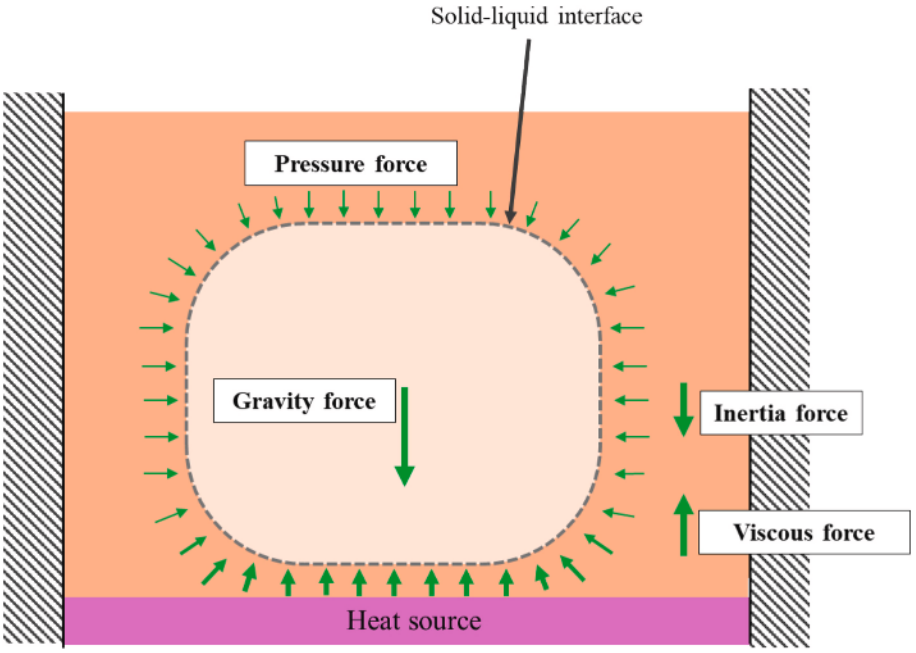


Fig. 4. Typical forces of pressure, gravity, viscous, and inertia, to be evaluated for the force balance equation on the solid region.

enthalpy-porosity technique. A solid velocity is first assumed which would predict the solid's position, after which the governing flow and energy equations are solved. The force balance acting on the solid body is then evaluated, and the guessed solid velocity is iteratively updated until convergence. The solid motion has to be determined externally through an iterative force-balance procedure, with the melt interface repeatedly reconstructed from the assumed solid velocity, with the limitation being that the predicted liquid fraction field obtained from an initial guessed solid velocity can be non-physical, requiring additional corrective treatments.

Kozak et al. [34] worked on a constrained shell-and-fin geometry while presenting an interesting novel and validated numerical method. The key modelling simplification is that once the conditions for sinking were judged to be satisfied, the computational cells corresponding to the solid region were explicitly shifted downward by one layer in order to preserve the thin melt layer required for CCM. The enthalpy contained in the displaced cells was then transported to the fluid region above the descending solid block. The work by Kozak and Ziskind [45] can be viewed as a direct continuation and refinement of the previous framework. The main advance is a more rigorous treatment of the interaction between the descending solid PCM and the surrounding melt. The model aims to recover the corresponding velocity and pressure fields

throughout the entire domain using Lagrangian markers on the underlying Eulerian grid. Forcing functions were then applied at the interface within the momentum equations, effectively imposing the "pushing" action of the solid onto the melt. This procedure enabled a revised velocity and pressure field to be obtained, from which a more accurate buoyancy force could be evaluated and returned to the force balance for the following time step.

A direct continuation of this line of work was later presented by Shockner and Ziskind [46], who retained the same general framework but further formalised the method using immersed boundary method (IBM). The solid PCM was still treated as a rigid body whose settling velocity was determined from a force balance, and its downward motion was imposed over each time step. A notable contribution of this work is the care taken in the time and spatial discretisation of both the momentum and energy equations. The transient terms are discretised using a hybrid implicit–explicit strategy, combining Crank–Nicolson treatment for linear diffusion terms with Adams–Bashforth discretisation for the non-linear convection terms in order to obtain second-order temporal accuracy. The work was later refined in [48] through detailed experimental validation, with the numerical model remaining the same.

Rozenfeld et al. [23] introduced an important variation to the developing CCM literature by demonstrating rotational solid motion rather than restricting it to translation in a single direction. This work considers the case of a cylindrical enclosure with fins that causes the solid chunk to rotate. The authors developed a hybrid analytical–numerical model specifically for the lower region of the enclosure, where CCM was expected to dominate along the vertical finned surface. The novelty of the study lies in the inclusion of both force and moment balance equations for the solid PCM. The shell resistance was represented through an additional close-contact melting layer that forms between the solid PCM and the heated enclosure wall. This model remains highly specialised to the assumed cylindrical finned geometry and relies on several simplifying assumptions, including quasi-steady melting, one-dimensional heat conduction across the thin liquid layer, laminar melt flow, negligible sensible heat within the film, and negligible shear stresses on the solid and fin surfaces.

Schüller and Kowalski [20] also represent a departure from the enthalpy-based CCM modelling tradition, in that they developed a numerical framework based on directly solving the reduced governing equations using finite differences in a Lagrangian reference frame. The study focuses on the related and more general problem of moving heat sources, allowing the model to capture both translational and rotational melting modes through the imposed motion of the thermal boundary conditions. This work's significance lies in its generalisation of prior CCM formulations to allow for spatially varying heat flux distributions at the heated surface. The momentum balance in the thin melt film is reduced to a Reynolds-type equation, which was then coupled to the energy equation through the melt velocity field.

A further development of this Lagrangian, moving-heat-source class of models was presented by Boledi et al. [49]. This approach incorporates the Stefan condition at the interface, such that the heat flux entering the melt film from the solid side becomes a time-dependent quantity obtained from the macro-scale temperature field. This study introduces more advanced discretisation and mesh-handling procedures than the earlier finite-difference Lagrangian approach. The transient temperature field in the solid was solved using a space–time finite element method (ST-FEM). The motion of the heat source was handled using a Virtual Region Shear-Slip Mesh Update Method (VR-SSMUM), which divides the mesh into stationary and moving regions to avoid repeated global remeshing and projection errors. The melt velocity was obtained from an external thin-film CCM model and used to update the mesh position iteratively at each time step. The study therefore retains the reduced-order melt-film approach of [20] while improving the robustness and transient consistency of the macroscopic thermal solution.

Kozak [47] presented another geometry-specific extension of CCM theory similar to that discussed with Rozenfeld et al. [23], where the governing equations were tailored to a particular physical configuration. In this case, the objective was to investigate how superhydrophobic surfaces influence close-contact melting, with particular attention given to the competing roles of hydrodynamic slip and thermal slip at the heated wall. The study is notable in that it moves beyond purely bulk mechanical considerations and instead examines how interfacial surface properties can modify the melt-film dynamics themselves. As with several earlier analytical and hybrid models, the motion of the solid region was not obtained from a full rigid-body momentum solution, but was instead treated implicitly through a reduced-order force balance. The resulting formulation produced a coupled set of first-order ordinary differential and nonlinear algebraic equations for the solid interface position and melt-film thickness.

Kozak [50] later considers another scenario-specific extension of CCM theory, focusing on melting over an isothermal surface without encapsulation, such that the molten phase is free to drain laterally from the contact region. A further consideration is that the liquid phase is no longer treated as a simple Newtonian melt; instead, the governing equations incorporate a Herschel–Bulkley rheology, allowing the model to account for yield-stress and shear-dependent viscosity effects within the draining liquid film. Under several assumptions, the model derives reduced momentum and heat-transfer equations for the Herschel–Bulkley melt, which are then rendered dimensionless to identify the key controlling groups.

A recent work by Shockner et al. [51] can be considered a continuation of [46,48] as it expands the established enthalpy framework they devised. This time they improve the stability of the advection of the solid phase and expand the force balance equation to allow for three degrees of freedom. This is achieved by advecting the solid region by the determined set velocity using the Volume of Fluid algorithm, which is well-known for its ability to handle and maintain a sharp interface using a bounded phase-fraction transport equation on the Eulerian grid. In contrast to the earlier immersed-boundary formulations, where the rigid-body displacement of the solid was imposed more directly after the force balance was evaluated, the use of VOF allows the solid PCM region to be translated and rotated in a numerically smoother and more stable manner while still preserving a sharp interface between the solid and surrounding liquid.

A major strength of the study is that it moves closer to a truly general computational treatment of encapsulated CCM, rather than relying on highly geometry-specific reduced equations or explicit cell-shifting procedures. The extension to rotational motion, together with stable VOF advection of the solid phase, makes it better suited to realistic confined melting configurations.

Established CFD platforms have been used for CCM studies through empirical parameter calibration or by coupling solid-force balances to the flow and energy equations. The following discussion includes both commercial software and the open-source OpenFOAM framework. These studies are synthesised in Table 5 in terms of validation, reported accuracy and geometric configuration.

Pan et al. [18] examine how far the standard enthalpy-porosity model in ANSYS Fluent can be pushed through careful calibration of its internal tuning parameters. Their simulations were carried out using a VOF description of the PCM–air system together with Fluent's default enthalpy-porosity method for melting. The main contribution is to investigate the appropriateness of modifying the mushy zone constant to match experimentally observed melting behaviour. Results show that the optimal value of this parameter depends strongly on the imposed driving temperature difference, and they further propose a linear correlation for selecting it across the tested conditions. A continuation of the tuning approach can be seen with Baghaei Oskouei et al. [53]. They show that for CCM-like settling in their latent thermal energy storage geometry, the required mushy zone constant can be estimated more systematically by examining the momentum equation in the vertical direction and assuming a representative settling velocity for the

remaining solid PCM. In this way, the unknown constant, C, is not selected only by trial-and-error fitting to experiments, but may be linked back to the force balance implied by the desired sinking behaviour. Work by Van Riet et al. [56] also explored tuning the mushy-zone constant and concluded the extreme difficulty in obtaining reliable results.

Faden et al. [52] incorporated a solid-settling treatment within the open-source CFD framework OpenFOAM, while still retaining the general fixed-grid structure of enthalpy-porosity and VOF-based phase tracking. A key contribution is the introduction of an implicit algorithm for the settling of the remaining solid PCM, in which the settling velocity is first obtained from a force balance and then imposed in the momentum equations through an extended Darcy source term. This is intended to improve numerical stability relative to earlier explicit settling-velocity approaches, particularly under larger temperature gradients where oscillations can become severe.

The model does not appear to solve the rigid-body motion of the solid as a fully separate immersed object implemented through momentum source terms (forcing functions) at the immersed-boundary interface. Rather, the solid–liquid interface is identified from the phase field, with a high VOF threshold used to determine which cells are treated as belonging to the solid region, and the calculated settling velocity is then prescribed through the Darcy-type momentum sink/source treatment. Based on this description, the role of the immersed boundary treatment seems to be limited mainly to defining the effective solid interface and its advection through the VOF algorithm, while the actual solid motion is enforced implicitly through the extended Darcy term. This is similar to the approach previously discussed with [51]. The work represents an important step in the use of openly accessible CFD tools for CCM-like settling problems.

A closely related strategy was later adopted by Huang et al. [54], who effectively translated the same general methodology into the COMSOL environment for a different application of a two-dimensional axisymmetric finned latent heat storage unit. As with Faden et al. [52], the model retains a fixed-grid formulation in which the energy equation is solved first, a sinking condition is checked, the solid–liquid interface is identified, and the settling velocity of the remaining solid PCM is then obtained from a force balance and incorporated back into the momentum equations through a source-term treatment. The main difference therefore is in the software platform and geometry considered. Huang et al. [54] extend the approach and place greater emphasis on the combined roles of solid conduction, natural convection, and solid PCM motion, while using iterative solution control, adaptive meshing, and refined time stepping to improve convergence and accuracy.

A further refinement of this work was presented by Huang et al. [57] with improved robustness through more advanced interface-tracking and meshing procedures. As in their earlier study, the remaining solid PCM velocity is still obtained from a quasi-static force balance and coupled back into the momentum equations through a source-term correction, but greater attention is given here to accurately extracting the evolving solid contour in more complex container geometries. In particular, the solid–liquid boundary is identified using a sharp-interface criterion based on a liquid fraction threshold of 0.85, which is slightly less restrictive than the 0.95 threshold used by Faden et al. [52], and is paired with an alpha-shape-based contour reconstruction method to improve smoothness and stability of the detected interface. Together with refined discretisation, boundary-dimension treatment, and more carefully controlled numerical updating, this makes the model a more mature implementation of the same underlying methodology rather than a fundamentally new approach.

Tian et al. [55] proposed a distinctly different Fluent-based route for simulating CCM by avoiding explicit force-balance settling algorithms and instead reformulating the problem entirely within an Eulerian multiphase framework. In their model, the VOF method is used to sharply distinguish the phases, providing a similar interface-capturing advantage to that discussed earlier [51]. However, rather than relying on enthalpy-porosity with a prescribed sinking velocity, phase change is handled through a mass transfer function that updates the phase distribution across the solid–liquid interface. The central novelty is then the treatment of the remaining "solid" PCM as a Bingham fluid within ANSYS Fluent. Within Fluent's internal modelling, the solid region is assigned a very high apparent viscosity when the local stress remains below a specified threshold, thereby effectively suppressing motion, while above that threshold the apparent viscosity decreases sufficiently to permit the region to move as though it were a yielded material. In this way, rigid-body-like descent is approximated without being explicitly solved.

This is an attractive idea because it keeps the entire CCM process inside a commercially available CFD framework and avoids some of the algorithmic complexity associated with interface forcing or sequential solid-translation procedures. However, the method introduces a different set of limitations. The yield or stress threshold required to trigger motion is not obvious and must be calibrated carefully, meaning that the onset of solid movement remains partly model-dependent rather than fully predictive. The approach assumes that a sufficiently high apparent viscosity will cause the yielded "solid" to move in a rigid-body-like manner, even though this is not guaranteed by the formulation itself, since the solid is still mathematically treated as a fluid, and deformation may not always be fully prevented. An inherent peculiarity is the need to initialise the problem with a thin liquid layer surrounding the solid region, which is required to enable the interface treatment and movement mechanism to function properly.

Sahray et al. [39] developed a different Fluent-based correction for gravity-driven CCM of a cylindrical PCM block on an isothermal horizontal surface, with the block surrounded by air and the melt free to drain laterally along the plate. The two-dimensional axisymmetric model retains a high mushy-zone parameter of 10^8 and supplements the axial momentum equation with a phase-weighted body-force source. A dynamically updated, smoothed correction factor compares the pressure required to support the remaining solid weight with the simulated mean pressure in the underlying melt film. Unlike Faden et al. [52], the method corrects the driving source rather than imposing a separately calculated common settling velocity. The coupled level-set/VOF model captures the PCM–air boundary, while the enthalpy–porosity liquid fraction describes the solid–liquid transition. Comparisons with the authors' Field's Metal and n-octacosane experiments and published CCM benchmarks support coherent descent and melting-rate predictions in the tested configurations.

The subsequent study by Sahray et al. [60] extends the pressure-corrected momentum-source approach to externally loaded melting inside a vertical cylindrical capsule. The model couples enthalpy–porosity melting to heat conduction through the capsule walls and a dynamically meshed piston, whose translation is specified through a user-defined motion function with mesh smoothing and remeshing. An important extension is the treatment of confinement; the liquid squeezed from beneath the solid must drain upward through the annular clearances and accumulate above the piston, generating back pressure that enters the coupled force and heat balances. For the investigated heat fluxes of 4–12 W cm^{-2} and external-load-to-initial-PCM-mass ratios of 2–12, increased loading primarily reduces melt-film thermal resistance and base temperature; under imposed heat flux, the overall melting rate remains mainly controlled by the supplied energy.

Across custom-built solvers and established CFD platforms, the reviewed approaches increasingly couple melt flow, phase change and solid motion. Agreement with experiments must nevertheless be interpreted in relation to each model's assumptions, calibration and validation configuration. The recent pressure-corrected source formulations [39,60] provide an additional route within commercial software and should be distinguished from both empirical mushy-zone tuning and force-balance methods that directly prescribe a settling velocity.

Pressure-enhanced CCM is therefore no longer absent from numerical modelling. Sahray et al. [60] explicitly couple externally loaded

melting with piston motion, melt redistribution and capsule-wall heat transfer. The remaining gap is broader validation of such coupled models, particularly under rapidly changing loads, across geometries and through complete operating cycles. Progress should be assessed through conservation, interface and solid-motion accuracy, and demonstrated transferability rather than the choice of software platform alone.

Table 6 compares the principal modelling approaches described above to support method selection. The comparison separates physical treatment from software platform: a commercial package can host different solid-motion models, while an open-source platform may require substantial custom development. Computational-cost entries indicate the work implied by each formulation, not measured rankings; the reviewed studies do not provide a common runtime benchmark. Validation is reported for the particular studies and configurations, and calibration against an experiment is not treated as evidence of transferability to other conditions.

4. Experimental developments

4.1. Background to experimental setup

Designing and operating experimental rigs for CCM requires careful consideration of both the geometry of the test vessel and the means of handling the liquid phase that develops during melting. Most studies employ vessels in the form of vertical cylinders [12,15,38,48,61–64] or shell-and-tube style heat exchangers [23,34,65,66], as these geometries provide well-defined contact areas and controlled boundary conditions for assessing melting behaviour. Heat is typically supplied through a heated base plate, thermal bath, heat-transfer fluid, GaN (Gallium Nitride) or Silicon device, ensuring a constant temperature or heat flux at the melt interface.

A key challenge in CCM experiments is how to manage the molten PCM that accumulates at the contact interface. Two principal strategies are observed in the literature. First is to allow the melt to rise alongside walls. Here, the PCM is allowed to flow upward around the solid block as melting proceeds. To enable this, the solid PCM must either be physically decoupled from the container wall (via a clearance gap) or preheated to create a thin pre-melted layer near the wall [62], preventing

Table 6
Qualitative comparison of CCM modelling approaches and practical selection considerations.

Approach / examples	Solid-body motion	Computational-cost considerations	User accessibility	Validation status	Geometry, typical use and main limitation
Custom thin-film / reduced-order models [20,23,34,47,50]	Motion follows reduced force/moment balances and the Stefan condition; translation or rotation is restricted by the assumed geometry.	Thin-film reduction limits the solved domain; nonlinear iteration may remain. Common timings are not reported.	Requires implementation of specialised equations; no general software workflow is established.	Experiments support selected configurations [23,34,50]; validation is not uniform across the group.	Best for idealised plates, cylinders and finned sectors, parameter studies and scaling. Transfer to other geometries requires re-derivation.
Custom CFD–rigid-body coupling [45,46,48,51]	Force-based solid motion is coupled to the melt through IBM; VOF advection in [51] enables planar translation and rotation.	Resolves flow and energy with interface forcing and thin-film resolution; coupling iterations add work. Not benchmarked.	High implementation effort; code availability and reproducibility must be checked study by study.	Experimental comparisons are reported [45,46,48,51]; accuracy may vary with melting stage.	Suitable for encapsulated CCM and asymmetric heating where solid pose matters. Dimensionality and rigid-body assumptions remain study-specific.
Fluent mushy-zone calibration [18,53,56]	Reduced momentum damping permits sinking-like motion, but does not impose rigid-body kinematics.	Uses an established solver workflow; repeated calibration and convergence checks add case-dependent work.	Accessible commercial interface, subject to licence access and careful parameter selection.	Fitted agreement is reported [18,53]; deformation and transferability limitations are identified [56].	Useful for calibrated storage-geometry studies. A fitted constant is not evidence of predictive solid motion in a new configuration.
Variable-viscosity / Bingham representations [43,55]	A high-viscosity or yield-stress material approximates the solid. Rigidity is not enforced by a separate body constraint.	Large coefficient contrasts and constitutive iterations can increase convergence effort; no common timings are available.	Implemented within OpenFOAM [43] or Fluent [55]; requires constitutive and phase-change settings.	Comparisons with experiments are reported for selected cases [43,55], not a universal viscosity or yield threshold.	Potentially useful when aggregate melting performance is prioritised. Shape-sensitive contact and rotation require separate verification.
OpenFOAM implicit settling [52]	A solid-force balance supplies settling velocity, imposed through an extended Darcy term on a fixed grid.	Coupled settling and pressure–velocity iterations are required. Common runtime comparisons are unavailable.	Open-source platform; implementation and solver customisation require specialist coding.	Validated against macrocapsule melting/settling experiments; Table 5 records the reported error measure.	Demonstrated for a rectangular capsule. Useful for gravity-driven settling; broader geometries and loading require further validation.
COMSOL force-balance coupling [54,57]	Quasi-static settling is linked to the momentum source; a phase-fraction contour identifies the solid.	Interface extraction, mesh refinement and coupled iteration determine workload; not benchmarked across studies.	Commercial multiphysics environment combined with custom routines and contour settings.	Validated in the reported finned and rectangular configurations; no general cross-geometry validation is established.	Applied to axisymmetric finned units and rectangular containers. Quasi-static motion and contour criteria constrain extrapolation.
Fluent pressure-corrected axial source [39]	High mushy-zone damping is retained; a pressure-based correction adjusts the solid-weighted axial driving source. No separate rigid-body velocity is prescribed.	Thin-film resolution and source-correction convergence dominate effort. Baseline: about 1.5 million cells and a 5 ms step; not a cross-method cost benchmark.	Commercial Fluent plus UDFs; major source-correction routines and settings are supplied.	Own Field's Metal/n-octacosane experiments and published CCM benchmarks; evidence is configuration-specific.	Open cylindrical block, 2D axisymmetry, gravity-driven descent. General rotation and strongly varying loads require further verification.
Fluent pressure-corrected source + dynamic piston mesh [60]	A solid-weighted axial source accounts for loading; prescribed UDF piston translation is coupled to melt drainage and back pressure.	Fine bottom/side films plus smoothing/remeshing of a coarser core; boundary-motion time-step restriction. No common runtime benchmark.	Commercial Fluent with custom momentum and piston-motion UDFs and dynamic-mesh configuration.	Two gravity-driven capsule benchmarks. No direct experimental validation of the externally loaded moving-piston case is reported.	2D axisymmetric conductive capsule. Initial liquid clearances aid start-up; correlations describe the later quasi-steady regime, not a complete cycle.

it from anchoring to the sides. Another way to decouple the solid bulk of PCM is mentioned in the literature, which is to allow the piston in the pressure-enhanced case to provide enough force to overcome the adhesion to the wall (mentioned in suppl. notes [15]). However, not enough experimental exploration has been performed for this approach. A summary of pressure-enhanced CCM systems is shown in Fig. 5.

The second option to manage the liquid phase is by draining the molten PCM [15,38]. Liquid PCM may be extracted through an opening near the heat source and allowed to freely deposit, typically when conducting performance analysis, or ideally transported to a separate container. This method can, in principle, sustain prolonged CCM without accumulation of a melt layer, but to-date the literature has not demonstrated a fully functional device for real-world applications using this drain-out approach.

Instrumentation for CCM experiments must provide both thermal and visual diagnostics. Thermocouples are widely used to track the temperature distribution around the heat source. To capture the evolution of the melt front, researchers often use transparent vessels, commonly Pyrex glass, enabling direct observation of phase boundary movement. High-speed or time-lapse imaging provides estimates of the melt fraction and solid sinking velocity. Digital image processing is applied for thermal imaging to observe temperature profiles and melt film analysis.

In thermal management experiments involving PCM-based heat sinks, the heat source is typically either an electric heating pad or a power-dissipating electronic device, such as a silicon or GaN component, with a known power input, seen in Fig. 6. Accurately determining the heat flux entering the PCM device is essential for validating thermal performance. When heat pads are used, convective and radiative losses to ambient air are often neglected. Instead, the heat flux escaping into the insulation beneath the pad is estimated by embedding multiple thermocouples within the insulation and applying transient one-dimensional heat conduction analysis, such as the Taylor series expansion of the temperature profile. The net heat input into the PCM heat sink system is then obtained by subtracting this calculated loss from the total supplied power. In contrast, when using an active electronic component as the heat source, surface heat losses to ambient air must be considered. These are typically estimated using the temperature difference between the device junction and the surrounding air, combined with an appropriate convective heat transfer coefficient, to yield the effective heat flux entering the thermal management unit.

These rigs establish the foundation for CCM testing, though challenges remain in scaling results to practical devices and in developing methods that can support continuous and application-ready operation.

4.2. Recent experimental approaches

Experimental investigations into gravity-driven CCM typically focus on small to moderately scaled systems, with PCM enclosures ranging from compact capsules (e.g., 12 mm × 11 mm [64]) to shell-and-tube geometries with lengths around 200 mm and diameters under 50 mm [65,66]. The majority of studies utilise simple cylindrical or rectangular enclosures [19,23,48], with occasional exploration of finned configurations or capsules with varied cross-sections to enhance thermal performance [34,67]. These setups aim to emulate practical configurations for thermal energy storage or thermal management systems, while maintaining geometric simplicity for experimental control and numerical validation.

Across the studies, the PCM materials selected tend to be medium-to-low melting temperature organic compounds such as n-eicosane ($T_m \approx 36.7$ °C) [19,23,34,48], 1-tetradecanol (Tm ≈ 37 °C) [57,65], and n-octadecane (Tm ≈ 28 °C) [25,67,68] with some extensions into nano-enhanced PCMs to study their conductivity and viscosity effects [64]. This range of melting temperatures positions the materials as suitable candidates for low-to-medium temperature applications, such as electronics cooling and low-grade heat recovery.

The heat input in these studies is generally supplied either via a thermal fluid (e.g., hot water) circulated at controlled temperatures ranging from ~50 °C to 70 °C [48,66], or through direct thermal contact using electrical heaters or copper hot plates [64]. Ambient bath

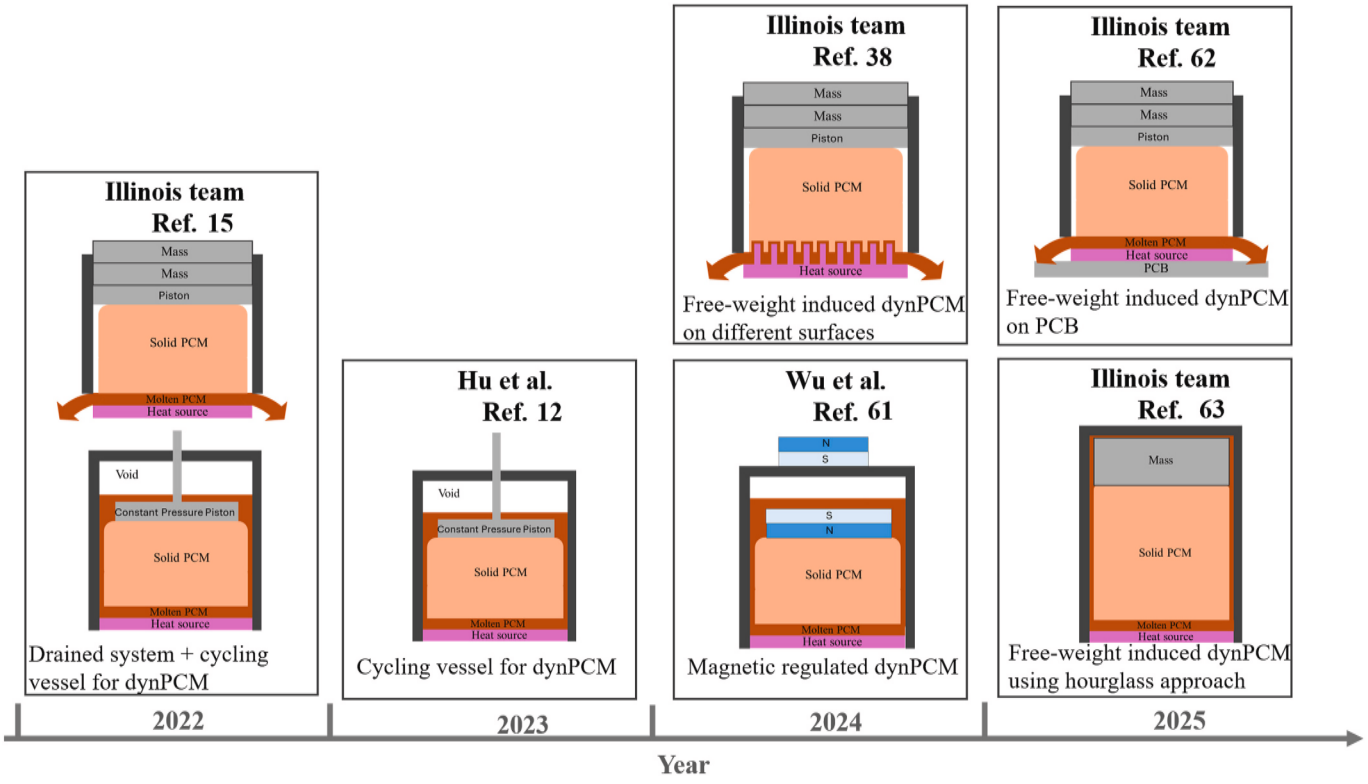


Fig. 5. Experimental configurations for pressure-enhanced CCM (heat source also represents hot plate or other heat spreader for simplification).

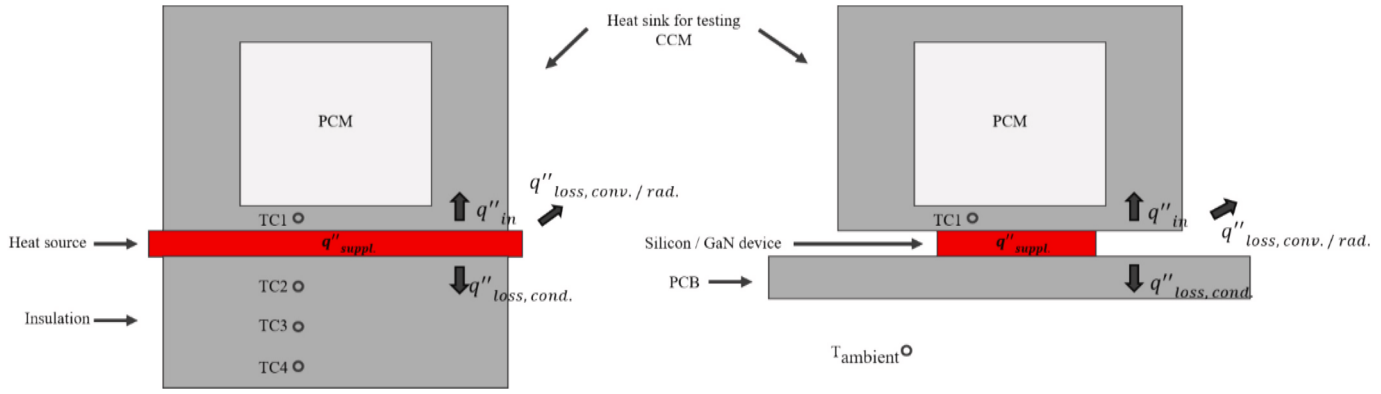


Fig. 6. Typical experimental setups for thermal management solutions.

conditions ranging from 20 °C above T_m up to 120 °C were also employed in capsule studies [25,67,68] to simulate natural convection conditions with minimal complexity.

In terms of performance, the adoption of CCM mechanisms led to substantial reductions in melting time compared to convective melting. Studies consistently reported melting time reductions by factors of ~2 to 2.5× when CCM was allowed, highlighting its effectiveness in accelerating phase change [23,34]. Moreover, volumetric power densities (Pv) up to 0.534 W/cm^3 were reported in high-performance configurations [66]. Interestingly, nano-enhanced PCMs demonstrated mixed results. While 1 wt% graphene nanoplatelets accelerated melting due to improved thermal conductivity, higher loadings (3 wt%) hindered performance due to increased viscosity and reduced melt film mobility [64].

Based on the pressure-enhanced CCM studies, a number of common experimental trends emerge that distinguish this approach from gravity-driven counterparts. Most notably, nearly all investigations employed paraffin wax as the PCM due to its consistent melting behaviour and manageable thermal properties, though some studies also tested low-melting-point metal alloys for comparison [12,61]. The experimental configurations predominantly featured vertical cylindrical geometries with heated base plates, providing controlled conditions for studying pressure-enhanced CCM rather than demonstrating that these geometries are required or optimal.

The geometric scales varied moderately, with cylinder diameters typically between 30 mm and 70 mm, and lengths between 60 mm and 215 mm. These results involve different materials, thermal boundary conditions and performance definitions and are not directly interchangeable. Thermal resistances were frequently reduced to the order of 10–4 K·m2/W [61], and peak power densities of up to 1.95 W/cm2 (areal power density) and 0.8 W/cm3 were reported under controlled pressure and heat flux conditions [15,61]. The up-to-fourfold enhancement cited in this review is the maximum reported under specific experimental conditions, not a normalised comparison across these studies or a general performance characteristic of pressure-enhanced CCM. A summary of the experimental contributions is presented in Table 7.

While the volume of experimental studies on pressure-enhanced CCM remains limited compared to gravity-driven CCM, the promising thermal performance results strongly indicate its potential for high-demand applications, especially where compact, low duty cycle, and fast-responding thermal control is critical.

To compare the diverse results in Table 7, Table 8 reports area-normalised thermal resistance for studies wherever the reported experimental inputs permit reconstruction. The selected cases generally use the highest jointly documented added load and thermal input, or HTF temperature, for the stated configuration. The common metric is

$$R_A = \frac{A_{ref}(T_{hot} - T_m)}{\dot{Q}_{basis}} = \frac{T_{hot} - T_m}{q''_{ref}} \tag{8}$$

Here, T_{hot} identifies the reported temperature plane, T_m is the study's melting-temperature reference, and the reference heat flux is the adopted heat rate divided by A_{ref}. The heat rate may be net heat input, nominal heater power or a reported stored-energy rate. R_A has units of K m^2/W. Area normalisation removes the explicit inverse-area factor in conventional thermal resistance, but not the effects of geometry, material, heat losses or temperature-measurement location.

Added nominal pressure is defined as $p_{nom} = F_{added}/A_{PCM}$. Zero denotes no added load, not zero gravitational driving force. Lower R_A indicates a smaller temperature excess at a given reference heat flux only when the measurement and heat-flow bases are comparable.

5. Discussion

5.1. Review of numerical and experimental approaches

Across the various studies, a predominant pattern is the heavy reliance on geometry-specific modelling. Whether through semi-analytical solutions rooted in the Stefan problem or numerical simulations built using custom code or commercial software, most methodologies are tailored to specific configurations, such as flat plates, spherical enclosures, or cylindrical tubes. Numerical models often remain confined within individual studies due to their complexity, limited publication, or restricted scale and scenario. Experimental work reflects this trend as well, with most investigations conducted within enclosed systems using gravity-driven CCM, where melting occurs vertically, causing the liquid phase to rise along vessel walls rather than being actively removed. A unifying challenge across all domains is the small scale of investigation, typically ranging from a few centimetres up to about 30 cm and rarely exceeding modest pressure loads, with 7.5–12.5 kPa being the most common upper limit explored in most studies. The predominance of simple geometries and low- to medium-temperature organic PCMs makes these findings most directly relevant to geometrically similar storage capsules, rather than to arbitrary devices. Transfer to electronics, cylindrical battery-cell assemblies or large-scale TES therefore requires application-specific checks of heat spreading, melt drainage, orientation, material operating range and repeatability; geometric similarity alone is insufficient.

The present synthesis does not establish a comparable validation base for high-temperature or molten-salt CCM, so its recommendations are not extrapolated to those systems. Volume expansion and PCM–air interfaces are considered where included in the reviewed models (Section 3); this is not a general assessment of reserved-gas behaviour or complete solidification–remelting cycles.

For applications limited by contact-film resistance, pressure-

Table 7
Experiments on CCM and performance.

No #	Ref.	Year	GD-CCM	Pressure enhanced CCM	Material	T_m	Shape / size	Heat applied	Performance achieved
1	[67]	1991	☒	☐	n-Octadecane ice	~27.8 °C 0 °C	Horizontal rectangular capsules, 100 mm length, 50.7 × 50.7 mm and 30.8 × 90.4 mm cross section	Ambient Bath Temperature up to 20 °C + T_m	*Rectangular capsules offer more stable and consistent heat storage rates during melting, making them preferable to cylindrical capsules for applications requiring steady thermal output*
2	[25]	1993	☒	☐	n-Octadecane	~28 °C	Horizontal cylindrical capsules, 0.04 to 0.2 m ⌀	Ambient Bath Temperature up to 70 °C	*Natural convection only contributes ~ 10–15% of the total heat transfer at low Stefan numbers*
3	[68]	1996	☒	☐	n-Octadecane	~28 °C	Spherical Capsule 90 mm outer ⌀, Cylindrical Capsule 150 mm length	Ambient Bath Temperature ~ 75–120 °C	*A considerable difference between the theoretical and experimental results for molten mass fraction in terms of a single dimensionless parameter*
4	[34]	2014	☒	☐	n-Eicosane	36.7 °C	Horizontal finned cylindrical enclosure, 218 mm length, 12 mm inner ⌀ and 44 mm outer ⌀ (PCM)	HTF Temperature: up to 67 °C	Melting time reduced by ~2.5 times with CCM
5	[23]	2015	☒	☐	n-Eicosane	36.7 °C	Horizontal finned cylindrical enclosure, 218 mm length, 12 mm inner ⌀ and 44 mm outer ⌀ (PCM)	HTF Temperature: 56.7 °C	CCM vs. Regular Melting: In the lower part of the unit, melting time was reduced by 2.5× when CCM was allowed
6	[64]	2018	☒	☐	Nano Enhanced 1-Tetradecanol (Graphene nanoplatelets)	37 °C	Vertical Cylinder 12 mm height × 11 mm ⌀ on copper plate	57 °C - 67 °C hot plate	1 wt% NePCM → Faster melting than pure PCM (0 wt%) due to higher thermal conductivity 3 wt% NePCM → Slower melting due to increased viscosity and film thickness, despite highest conductivity
7	[65]	2022	☒	☐	1-Tetradecanol	37 °C	Shell-and-tube TES unit 200 mm length 49 mm diameter	*heat source of 67 °C*	P_V up to 0.455 W/cm^3
8	[15]	2022	☒	☒	Paraffin Wax	55 °C	Vertical Cylinder 40 × 40 mm^2 base plate	q" = 3 kW cm^{-2}	$E_V = 230\,J\,cm^{-3}$ $P_V = 0.8\,W\,cm^{-3}$
9	[48]	2023	☒	☐	n-Eicosane	36.7 °C	Vertical cylindrical capsule 62.2 mm height × inner diameter 62.2 mm ⌀ on Aluminium plate	1. Peripheral heating with HTF: up to ~67 °C 2. Bottom heating via Thermofoil electric heater: up to 30 W	Using CCM shows sharper top interface, faster melting vs. convective-only (HTF) cases
10	[66]	2023	☒	☐	1-Tetradecanol	37 °C	Vertical shell-and-tube with annular fins Length: 200 mm. 49 mm ⌀	Heat Transfer Fluid: Water at 67 °C	$P_V = 0.534\,W\,cm^{-3}$
11	[19]	2023	☒	☐	n-Eicosane	36.4–37.9 °C	Rectangular enclosure with and without fins 126 × 60 × 100 mm	HTF: Water at 50 °C, 55 °C, and 60 °C	CCM reduced melting time by 42–50% over constrained melting (no-fin case, horizontal)
12	[12]	2023	☒	☒	Paraffin wax Low Melting Point Alloy	55.7 °C 60.3 °C	Vertical Cylinder 70 mm ⌀, 60 mm length + Copper Foam	5000 W/m^2 to 25,000 W/m^2	**Paraffin**: plateau temperature of ~ T_m Thermal Resistance reduced to <2.5 × 10^{-4} K·m^2/W **LMPA**: plateau temperature of ~ T_m Thermal Resistance reduced to <1 × 10^{-4} K·m^2/W
13	[61]	2024	☐	☒	Paraffin wax Bi-In-Pb-Sn Alloy	42–44 °C 47 °C	Cylindrical Copper Vessel 30 mm ⌀, 80 mm length	0.4–3.0 W/cm^2	P_{areal} ~ 1.95 W cm^{-2} Thermal Resistance reduced to <4.5 × 10^{-4} K·m^2/W
14	[38]	2024	☒	☒	Paraffin Wax	58 °C	Vertical Cylinder Projected Area of 14.5 cm^2	1.4 W/cm^2 to 4.5 W/cm^2	plateau temperature of ~6 °C above T_m 157% higher thermal conductance with extended surfaces
15	[62]	2025	☒	☒	Eicosane (C20H42)	36.7 °C	Vertical Cylinder 44 mm ⌀, 215 mm length	3.8 W/cm^2	with 500 g weight: ~8 °C above T_m
16	[63]	2025	☒	☒	Paraffin Wax	58 °C	Vertical Cylinder 3.4 cm × 6.5 cm base plate	4.4 W/cm^2 to 46.6 W/cm^2	stable junction temperatures at ~58 °C

Table 8
Area-normalised resistance at selected operating conditions for studies of Table 7.

No. #	Ref.	Year	Added p_{nom} (kPa)	R_A (10^{-4} K m^2/W)
1	[65]	2022	0	≈20.2
2	[15]	2022	6.40	≈3.9
3	[66]	2023	0	≈19.0
4	[19]	2023	0	≈25.9
5	[12]	2023	0 / 2.25 (GD / PE)	Paraffin: ≈10.9 / 3.3 LMPA: ≈3.08 / 0.7
6	[62]	2025	3.23	≈4.8
7	[63]	2025	7.50	≈10.2

Notes. Values are rounded reconstructions or explicitly labelled reported values, not a common uncertainty-controlled ranking. GD / PE pairs in study 12 use the same material and imposed heat flux.

enhanced CCM is a promising development direction rather than a necessary replacement for gravity-driven designs. Enhancements approaching fourfold apply to particular experimental conditions (Section 4.2), and their transfer to other systems remains to be demonstrated. Appropriate melt drainage and controlled loading are therefore development priorities rather than guarantees of improved device performance. Recent piston-driven modelling [60] advances this direction, although validation across operating conditions and device configurations remains limited.

While foundational research has provided valuable insights into various aspects of CCM, moving forward will require a combination of integrated, geometry-flexible models and larger-scale, pressure-tuned experiments that move beyond the constraints imposed by current setups.

5.2. *Perspectives on the potential widespread adoption of CCM technology*

Successful integration of CCM into real-world energy storage and thermal management systems hinges on both robust numerical modelling and strategic experimental design. The synthesis supports two complementary priorities: validated coupled modelling in accessible custom or established CFD platforms, and application-specific hardware prototyping.

Conventional fixed-grid implementations require an additional treatment of solid motion, as distinguished from parameter-selection and implementation errors in Section 3.2. A popular current workaround is to strategically un-suppress the velocity based on empirically derived data [18,56], or directly prescribe the settling velocity of the solid phase based on iteratively solving the force balance equation [52,57] or by using thin film lubrication theory.

A coupled CFD–multiphysics framework is a promising generalisable pathway rather than an established optimum for CCM. Several of the reviewed VOF, immersed-boundary, Lagrangian and custom-solver approaches already couple these processes and can remain suitable within their validated scope (Table 6). In such a framework, melt flow and heat transfer are coupled to the dynamics of the melting solid. For rapidly varying loads, transient coupling should preserve consistent interfacial mass, momentum and energy balances, with convergence of the coupled solution assessed within each time step. Either a partitioned or monolithic strategy may be used, as in fluid–structure interaction (FSI) modelling [69].

Unlike a non-melting FSI boundary, the PCM interface also recedes through phase change. Its coupling conditions must therefore account for mass transfer and latent heat, alongside momentum exchange and the changing mass and shape of the remaining solid. In particular, melting-interface velocity need not equal solid-material velocity in the normal direction; the interfacial mass balance relates these velocities to the melt velocity. Resolving this distinction consistently, together with energy transport and interface motion, is essential when extending CCM models to more demanding transient operation.

While numerical tools lay the groundwork, successful adoption of CCM depends on careful alignment with the performance constraints of specific applications. Two distinct trends emerge: the first being gravity-driven CCM for energy storage devices, and the second is pressure-enhanced CCM for thermal management.

In TES, where rapid charging is less critical, gravity-driven CCM provides a viable and low-complexity solution. Its inherent simplicity and passive operation make it attractive for integrating into shell-and-tube geometries, especially when space is constrained. However, to truly capitalise on its benefits, the CCM mechanism must be central to the system design, not an afterthought. Configurations that merely patch CCM into conventional setups fail to deliver meaningful performance gains.

For thermal management systems, extensive reviews have already covered PCM applications for low but constant power devices such as data centres [70,71]. In contrast, certain thermal management systems, in particular current and future electronic systems, demand high power densities and fast response times. Pressure-enhanced CCM is therefore a candidate for high-heat-flux applications, with the maximum reported enhancement of approximately fourfold (specific to the experimental conditions summarised in Section 4.2).

Pressure may help release adhered PCM and re-establish close-contact conditions, but the available evidence does not demonstrate reliable prevention of wall adhesion or repeatable melt-film regeneration over complete cycles. These remain engineering challenges to be tested alongside piston reset and re-solidification, rather than established advantages of pressure-enhanced CCM.

6. Conclusions

This review synthesises numerical and experimental developments in CCM for PCM-based TES and thermal management. The following conclusions distinguish established findings, emerging trends and proposed future directions:

- **Established finding.** CCM maintains a thin melt film between the solid PCM and the heated surface, providing a route to faster heat absorption than configurations in which a thicker liquid layer develops.
- **Established limitation.** Current modelling remains strongly dependent on geometry and assumptions. Thin-film and reduced-order formulations are useful for idealised configurations, but require additional treatment when bulk convection, complex geometry or transient solid motion becomes important.
- **Established limitation.** Empirically tuned momentum damping and variable-viscosity representations can reproduce selected melting responses, but agreement in melt fraction alone does not establish accurate rigid-body motion. Parameter sensitivity, solid deformation and convergence must also be assessed.
- **Emerging modelling trend.** Coupled flow, energy, phase-change and solid-motion formulations offer a promising generalisable pathway, including successful custom and established-software implementations. Their demonstrated accuracy remains configuration-specific; the available comparisons do not establish a universally superior framework.
- **Emerging experimental direction**. Gravity-driven CCM is a relatively simple option for suitable TES geometries, while pressure-enhanced CCM is a candidate for compact, high-heat-flux thermal management. The predominance of simple test geometries and organic PCMs, together with limited device-level and cyclic validation, prevents these recommendations from being generalised to all applications.
- **Proposed future directions**. Practical adoption requires validation beyond individual melting tests, including scale-up, consistent performance reporting, solid–wall interactions and repeatable reset and

re-solidification. These remain priorities for integrated modelling and device development.

7. Outlook and recommendations

The following priorities are proposed for researchers, industrial developers, and funding bodies:

- **Develop shared validation benchmarks.** Publish geometry, boundary conditions, material properties and uncertainty estimates together with temperature, melt-fraction and solid-position measurements, so that competing numerical approaches can be assessed against the same evidence.
- **Validate coupled modelling frameworks.** Test conservation, interface treatment and solid-motion predictions under transient loads before transferring calibrated models to new geometries. Make implementation details and verification cases available for both custom codes and established CFD platforms.
- **Standardise experimental performance reporting.** Report heat input, losses, PCM mass and volume, heated area, applied force or pressure and comparison baselines. These data are needed to distinguish material-, device- and load-dependent improvements.
- **Demonstrate repeatable device operation.** Evaluate melting, piston reset and re-solidification within representative duty cycles. Quantify reset time and energy demand, and document adhesion, leakage and repeatability rather than reporting a single successful melting event.
- **Support application-led scale-up.** Prioritise collaborative funding for transferable solvers, instrumented prototypes and long-duration testing. Assess thermal gains alongside actuator requirements, system mass, manufacturability and the intended TES or thermal-management operating conditions.

As a conceptual outlook, the authors propose piston-assisted CCM for intermittent electronics loads [72,73]. During a short high-power event, a piston could apply additional load to the solid PCM to reduce contact-film resistance. The cited studies motivate the application; they do not validate this proposed CCM operating sequence.

Reset would require sufficient time and heat-rejection capacity for piston retraction and PCM re-solidification; local interface reheating could be investigated if adhesion prevents retraction. Repeatability, reset time and energy penalties remain unvalidated for this concept and require cycle-resolved experiments.

CRediT authorship contribution statement

Daut Mustafic: Writing – original draft. **Fatma Al-widyan:** Supervision. **Nick S. Bennett:** Writing – review & editing. **Mohammad S. Islam:** Writing – review & editing.

Declaration of competing interest

The authors declare that they have no known competing financial interests or personal relationships that could have appeared to influence the work reported in this paper.

Acknowledgement

This research is supported by an Australian Government Research Training Program Scholarship.

Data availability

Data will be made available on request.

References

[1] A. Sharma, V.V. Tyagi, C.R. Chen, D. Buddhi, Review on thermal energy storage with phase change materials and applications, Renew. Sust. Energ. Rev. 13 (2) (Feb. 2009) 318–345, https://doi.org/10.1016/j.rser.2007.10.005.
[2] A.S. Fleischer, Cooling our insatiable demand for data, Science (1979) 370 (6518) (Nov. 2020) 783–784, https://doi.org/10.1126/science.abe5318.
[3] A.A. Kebede, T. Kalogiannis, J. Van Mierlo, M. Berecibar, A comprehensive review of stationary energy storage devices for large scale renewable energy sources grid integration, Renew. Sust. Energ. Rev. 159 (May 2022) 112213, https://doi.org/10.1016/j.rser.2022.112213.
[4] Y. Liu, R. Zheng, J. Li, High latent heat phase change materials (PCMs) with low melting temperature for thermal management and storage of electronic devices and power batteries: critical review, Renew. Sust. Energ. Rev. 168 (Oct. 2022) 112783, https://doi.org/10.1016/j.rser.2022.112783.
[5] B. Indulakshmi, G. Madhu, Heat transfer modeling and simulations for electronic cooling systems embedded with phase changing materials, *Heat Transfer–Asian Res.* 47 (1) (Jan. 2018) 185–202, https://doi.org/10.1002/htj.21298.
[6] Q. Wang, B. Jiang, B. Li, Y. Yan, A critical review of thermal management models and solutions of lithium-ion batteries for the development of pure electric vehicles, Renew. Sust. Energ. Rev. 64 (Oct. 2016) 106–128, https://doi.org/10.1016/j.rser.2016.05.033.
[7] H. Ami Ahmadi, N. Variji, A. Kaabinejadian, M. Moghimi, M. Siavashi, Optimal design and sensitivity analysis of energy storage for concentrated solar power plants using phase change material by gradient metal foams, J. Energy Storage 35 (Mar. 2021) 102233, https://doi.org/10.1016/j.est.2021.102233.
[8] Z. Khan, Z. Khan, A. Ghafoor, A review of performance enhancement of PCM based latent heat storage system within the context of materials, thermal stability and compatibility, Energy Convers. Manag. 115 (May 2016) 132–158, https://doi.org/10.1016/j.enconman.2016.02.045.
[9] A.M. Abdulateef, S. Mat, J. Abdulateef, K. Sopian, A.A.A. l-Abidi, Geometric and design parameters of fins employed for enhancing thermal energy storage systems: a review, Renew. Sust. Energ. Rev. 82 (Feb. 2018) 1620–1635, https://doi.org/10.1016/j.rser.2017.07.009.
[10] R.D. Weinstein, T.C. Kopec, A.S. Fleischer, E. D'Addio, C.A. Bessel, The experimental exploration of embedding phase change materials with graphite nanofibers for the thermal management of electronics, J. Heat Transf. 130 (4) (Apr. 2008), https://doi.org/10.1115/1.2818764.
[11] W.Q. Li, S.J. Guo, L. Tan, L.L. Liu, W. Ao, Heat transfer enhancement of nano-encapsulated phase change material (NEPCM) using metal foam for thermal energy storage, Int. J. Heat Mass Transf. 166 (Feb. 2021) 120737, https://doi.org/10.1016/j.ijheatmasstransfer.2020.120737.
[12] J. He, W. Chu, Q. Wang, Experimental study on pressure-enhanced close contact melting with PCMs for stable temperature control of high heat flux electronic devices, Appl. Therm. Eng. 230 (Jul. 2023) 120707, https://doi.org/10.1016/j.applthermaleng.2023.120707.
[13] A. Bejan, Contact Melting Heat Transfer and Lubrication, 1994, pp. 1–38, https://doi.org/10.1016/S0065-2717(08)70231-4.
[14] N. Hu, L.-W. Fan, X. Gao, H.A. Stone, Close-contact melting on hydrophobic textured surfaces: confinement and meniscus effects, J. Fluid Mech. 1010 (May 2025) A46, https://doi.org/10.1017/jfm.2025.385.
[15] W. Fu, X. Yan, Y. Gurumukhi, V.S. Garimella, W.P. King, N. Miljkovic, High power and energy density dynamic phase change materials using pressure-enhanced close contact melting, Nat. Energy 7 (3) (Mar. 2022) 270–280, https://doi.org/10.1038/s41560-022-00986-y.
[16] N. Hu, Z.-R. Li, Z.-W. Xu, L.-W. Fan, Rapid charging for latent heat thermal energy storage: a state-of-the-art review of close-contact melting, Renew. Sust. Energ. Rev. 155 (Mar. 2022) 111918, https://doi.org/10.1016/j.rser.2021.111918.
[17] H. Hong, A. Saito, Numerical method for direct contact melting in transient process, Int. J. Heat Mass Transf. 36 (8) (Jan. 1993) 2093–2103, https://doi.org/10.1016/S0017-9310(05)80140-1.
[18] C. Pan, et al., Experimental, numerical and analytic study of unconstrained melting in a vertical cylinder with a focus on mushy region effects, Int. J. Heat Mass Transf. 124 (Sep. 2018) 1015–1024, https://doi.org/10.1016/j.ijheatmasstransfer.2018.04.009.
[19] A. Abdi, H. Rastan, Experimental comparative analysis of close-contact and constrained melting of n-eicosane in a finned rectangular cavity, Appl. Therm. Eng. 219 (Jan. 2023) 119677, https://doi.org/10.1016/j.applthermaleng.2022.119677.
[20] K. Schüller, J. Kowalski, Spatially varying heat flux driven close-contact melting – a Lagrangian approach, Int. J. Heat Mass Transf. 115 (Dec. 2017) 1276–1287, https://doi.org/10.1016/j.ijheatmasstransfer.2017.08.092.
[21] Yaojiang Hu, Suyi Huang, Mingheng Shi, A generalized analysis of close-contact melting processes in two-dimensional axisymmetric geometries, Int. Commun. Heat Mass Transfer 26 (3) (Apr. 1999) 339–347, https://doi.org/10.1016/S0735-1933(99)00020-2.
[22] D. Groulx, M. Lacroix, Effects of convection and inertia on close contact melting, Int. J. Therm. Sci. 42 (12) (Dec. 2003) 1073–1080, https://doi.org/10.1016/S1290-0729(03)00096-6.
[23] T. Rozenfeld, Y. Kozak, R. Hayat, G. Ziskind, Close-contact melting in a horizontal cylindrical enclosure with longitudinal plate fins: demonstration, modeling and application to thermal storage, Int. J. Heat Mass Transf. 86 (Jul. 2015) 465–477, https://doi.org/10.1016/j.ijheatmasstransfer.2015.02.064.
[24] N. Hu, R.-H. Zhang, S.-T. Zhang, J. Liu, L.-W. Fan, A laser interferometric measurement on the melt film thickness during close-contact melting on an isothermally-heated horizontal plate, Int. J. Heat Mass Transf. 138 (Aug. 2019) 713–718, https://doi.org/10.1016/j.ijheatmasstransfer.2019.04.102.

[25] T. Saitoh, K. Kato, Experiment on melting in heat storage capsule with close contact and natural convection, Exp. Thermal Fluid Sci. 6 (3) (Apr. 1993) 273–281, https://doi.org/10.1016/0894-1777(93)90068-T.
[26] K.P. Sarath, M. Feroz Osman, R. Mukhesh, K.V. Manu, M. Deepu, A review of the recent advances in the heat transfer physics in latent heat storage systems, Thermal Science and Engineering Progress 42 (Jul. 2023) 101886, https://doi.org/10.1016/j.tsep.2023.101886.
[27] John Crank, Free and Moving Boundary Problems, Clarendon Press; Oxford University Press, 1984.
[28] M.K. Moallemi, R. Viskanta, Analysis of close-contact melting heat transfer, Int. J. Heat Mass Transf. 29 (6) (Jun. 1986) 855–867, https://doi.org/10.1016/0017-9310(86)90181-X.
[29] M.K. Moallemi, B.W. Webb, R. Viskanta, An experimental and analytical study of close-contact melting, J. Heat Transf. 108 (4) (Nov. 1986) 894–899, https://doi.org/10.1115/1.3247030.
[30] T.S. Saitoh, H. Hoshina, K. Yamada, Theoretical analysis and experiment on combined close-contact and natural convection melting in thermal energy storage spherical capsule, in: IECEC-97 Proceedings of the Thirty-Second Intersociety Energy Conversion Engineering Conference (Cat. No.97CH6203), IEEE, 1997, pp. 1656–1661, https://doi.org/10.1109/IECEC.1997.656670.
[31] T.S. Saitoh, A. Hoshi, Analysis of close-contact melting with inner wall temperature variation in a horizontal cylindrical capsule, in: IECEC-97 Proceedings of the Thirty-Second Intersociety Energy Conversion Engineering Conference (Cat. No.97CH6203), IEEE, 1997, pp. 1641–1645, https://doi.org/10.1109/IECEC.1997.656667.
[32] H. Yoo, Analytical solutions to the unsteady close-contact melting on a flat plate, Int. J. Heat Mass Transf. 43 (8) (Apr. 2000) 1457–1467, https://doi.org/10.1016/S0017-9310(99)00221-5.
[33] H. Yoo, Initial transient behavior during close-contact melting induced by convective heating, Int. J. Heat Mass Transf. 44 (11) (Jun. 2001) 2193–2197, https://doi.org/10.1016/S0017-9310(00)00233-7.
[34] Y. Kozak, T. Rozenfeld, G. Ziskind, Close-contact melting in vertical annular enclosures with a non-isothermal base: theoretical modeling and application to thermal storage, Int. J. Heat Mass Transf. 72 (May 2014) 114–127, https://doi.org/10.1016/j.ijheatmasstransfer.2013.12.058.
[35] V.S. Garimella, et al., Fundamental limits of dynamic phase change materials, Appl. Phys. Lett. 124 (12) (Mar. 2024), https://doi.org/10.1063/5.0190273.
[36] W.-B. Ye, M. Arıcı, Exploring mushy zone constant in enthalpy-porosity methodology for accurate modeling convection-diffusion solid-liquid phase change of calcium chloride hexahydrate, Int. Commun. Heat Mass Transfer 152 (Mar. 2024) 107294, https://doi.org/10.1016/j.icheatmasstransfer.2024.107294.
[37] M. Ezra, Y. Kozak, The influence of thermal convection in the thin molten layer on close-contact melting processes, Int. J. Heat Mass Transf. 235 (Dec. 2024) 126184, https://doi.org/10.1016/j.ijheatmasstransfer.2024.126184.
[38] R.A. Stavins, et al., Dynamic phase change materials with extended surfaces, Appl. Phys. Lett. 125 (6) (Aug. 2024), https://doi.org/10.1063/5.0217531.
[39] D. Sahray, et al., Close-contact melting of a cylindrical phase change material block on a heated surface, Int. J. Heat Mass Transf. 257 (Apr. 2026) 128175, https://doi.org/10.1016/j.ijheatmasstransfer.2025.128175.
[40] S.A. Prakash, C. Hariharan, R. Arivazhagan, R. Sheeja, V.A.A. Raj, R. Velraj, Review on numerical algorithms for melting and solidification studies and their implementation in general purpose computational fluid dynamic software, J. Energy Storage 36 (Apr. 2021) 102341, https://doi.org/10.1016/j.est.2021.102341.
[41] V.R. Voller, C.R. Swaminathan, General source-based method for solidification phase change, Numer. Heat Transf. B Fundam. 19 (2) (Jan. 1991) 175–189, https://doi.org/10.1080/10407799108944962.
[42] M. Salcudean, Z. Abdullah, On the numerical modelling of heat transfer during solidification processes, Int. J. Numer. Methods Eng. 25 (2) (Jun. 1988) 445–473, https://doi.org/10.1002/nme.1620250212.
[43] R.R. Kasibhatla, A. König-Haagen, F. Rösler, D. Brüggemann, Numerical modelling of melting and settling of an encapsulated PCM using variable viscosity, Heat Mass Transf. 53 (5) (May 2017) 1735–1744, https://doi.org/10.1007/s00231-016-1932-0.
[44] M. Giangi, F. Stella, T.A. Kowalewski, Phase change problems with free convection: fixed grid numerical simulation, Comput. Vis. Sci. 2 (2–3) (Dec. 1999) 123–130, https://doi.org/10.1007/s007910050034.
[45] Y. Kozak, G. Ziskind, Novel enthalpy method for modeling of PCM melting accompanied by sinking of the solid phase, Int. J. Heat Mass Transf. 112 (Sep. 2017) 568–586, https://doi.org/10.1016/j.ijheatmasstransfer.2017.04.088.
[46] T. Shockner, G. Ziskind, Combined close-contact and convective melting in a vertical cylindrical enclosure, Int. J. Heat Mass Transf. 177 (Oct. 2021) 121492, https://doi.org/10.1016/j.ijheatmasstransfer.2021.121492.
[47] Y. Kozak, Theoretical analysis of close-contact melting on superhydrophobic surfaces, J. Fluid Mech. 943 (Jul. 2022) A39, https://doi.org/10.1017/jfm.2022.458.
[48] T. Shockner, G. Ziskind, Experimental and numerical evaluation of phase-change material performance in a vertical cylindrical capsule for thermal energy storage, Appl. Therm. Eng. 219 (Jan. 2023) 119519, https://doi.org/10.1016/j.applthermaleng.2022.119519.
[49] L. Boledi, F. Key, B. Terschanski, S. Elgeti, J. Kowalski, A scale-coupled numerical method for transient close-contact melting, Comput. Math. Appl. 143 (Aug. 2023) 277–288, https://doi.org/10.1016/j.camwa.2023.05.011.
[50] Y. Kozak, Close-contact melting of a vertical cylinder on an isothermal surface: modeling and investigation for a non-Newtonian Herschel-Bulkley fluid liquid-phase, Int. J. Heat Mass Transf. 225 (Jun. 2024) 125378, https://doi.org/10.1016/j.ijheatmasstransfer.2024.125378.
[51] T. Shockner, et al., Simultaneous close-contact melting on two asymmetric surfaces: demonstration, modeling and application to thermal storage, Int. J. Heat Mass Transf. 232 (Nov. 2024) 125950, https://doi.org/10.1016/j.ijheatmasstransfer.2024.125950.
[52] M. Faden, A. König-Haagen, S. Höhlein, D. Brüggemann, An implicit algorithm for melting and settling of phase change material inside macrocapsules, Int. J. Heat Mass Transf. 117 (Feb. 2018) 757–767, https://doi.org/10.1016/j.ijheatmasstransfer.2017.10.033.
[53] S. Baghaei Oskouei, Z.-R. Li, Ö. Bayer, L.-W. Fan, Close-contact melting and natural convection in unconstrained melting: a parametric study, Int. J. Heat Mass Transf. 218 (Jan. 2024) 124795, https://doi.org/10.1016/j.ijheatmasstransfer.2023.124795.
[54] Y. Huang, P. Huang, Z. Deng, C. Zhang, Gravity-driven close contact melting heat transfer in gradient latent heat storage units, Int. Commun. Heat Mass Transfer 156 (Aug. 2024) 107687, https://doi.org/10.1016/j.icheatmasstransfer.2024.107687.
[55] S. Tian, B. Tan, Y. Lin, T. Wang, K. Hu, A Eulerian numerical model to predict the enhancement effect of the gravity-driven motion melting process for latent thermal energy storage, Entropy (Basel, Switzerland) 26 (2) (Feb. 2024) 175, https://doi.org/10.3390/e26020175.
[56] V. Van Riet, T. Shockner, W. Beyne, G. Ziskind, M. De Paepe, J. Degroote, Limitations of the enthalpy-porosity method for numerical simulation of close-contact melting on inclined surfaces, J. Phys. Conf. Ser. 2766 (1) (May 2024) 012214, https://doi.org/10.1088/1742-6596/2766/1/012214.
[57] Y. Huang, P. Huang, C. Yu, Close-contact melting enhancement mechanisms in space-constrained and large-space containers, Int. J. Heat Mass Transf. 237 (Feb. 2025) 126408, https://doi.org/10.1016/j.ijheatmasstransfer.2024.126408.
[58] A. Bejan, Single correlation for theoretical contact melting results in various geometries, Int. Commun. Heat Mass Transfer 19 (4) (Jul. 1992) 473–483, https://doi.org/10.1016/0735-1933(92)90003-Z.
[59] W. Chen, S. Cheng, Z. Luo, W. Gu, Study of contact melting inside isothermally heated vertical cylindrical capsules, J. Therm. Sci. 2 (3) (Sep. 1993) 190–195, https://doi.org/10.1007/BF02650856.
[60] D. Sahray, R.A. Stavins, B. Celebi, W.P. King, N. Miljkovic, G. Ziskind, Comprehensive modeling of external load-driven dynamic melting in a vertical cylindrical capsule, Int. J. Heat Mass Transf. 271 (Dec. 2026) 129247, https://doi.org/10.1016/j.ijheatmasstransfer.2026.129247.
[61] S. Wu, X. Zhang, K. Tang, T. Li, Magnetically- regulated close contact melting for high-power-density latent heat energy storage, J. Energy Storage 95 (Aug. 2024) 112660, https://doi.org/10.1016/j.est.2024.112660.
[62] I. Salman, et al., A 'hourglass' system for transient thermal management based on dynamic close-contact melting of a phase-change material, Int. J. Heat Mass Transf. 239 (Apr. 2025) 126542, https://doi.org/10.1016/j.ijheatmasstransfer.2024.126542.
[63] S. Kim, et al., Cooling high power electronics using dynamic phase change material, Int. J. Heat Mass Transf. 237 (Feb. 2025) 126433, https://doi.org/10.1016/j.ijheatmasstransfer.2024.126433.
[64] N. Hu, Z.-Q. Zhu, Z.-R. Li, J. Tu, L.-W. Fan, Close-contact melting heat transfer on a heated horizontal plate: revisited in the presence of nano-enhanced phase change materials (NePCM), Int. J. Heat Mass Transf. 124 (Sep. 2018) 794–799, https://doi.org/10.1016/j.ijheatmasstransfer.2018.03.089.
[65] Z.-R. Li, S. Baghaei Oskouei, G.-T. Fu, Ö. Bayer, L.-W. Fan, Enhanced power density during energy charging of a shell-and-tube thermal storage unit: comparison between the inclusion of metal fins and foams, J. Energy Storage 55 (Nov. 2022) 105576, https://doi.org/10.1016/j.est.2022.105576.
[66] Z.-R. Li, Z.-K. Zhang, X.-R. Wang, S.-S. Ni, L.-W. Fan, Synergistic enhancement strategy on the heat charging process of a shell-and-tube thermal storage device based on close-contact melting mechanism and nano-enhanced phase change material, J. Energy Storage 72 (Nov. 2023) 108529, https://doi.org/10.1016/j.est.2023.108529.
[67] T. Hirata, Y. Makino, Y. Kaneko, Analysis of close-contact melting for octadecane and ice inside isothermally heated horizontal rectangular capsule, Int. J. Heat Mass Transf. 34 (12) (Dec. 1991) 3097–3106, https://doi.org/10.1016/0017-9310(91)90079-T.
[68] T.S. Saitoh, A. Hoshi, Experimental investigation on combined close-contact and natural convection melting in horizontal cylindrical and spherical capsules, in: IECEC 96. Proceedings of the 31st Intersociety Energy Conversion Engineering Conference, IEEE, 1996, pp. 2090–2094, https://doi.org/10.1109/IECEC.1996.553452.
[69] Steffen Basting, et al., Fluid-Structure Interaction : Modeling, Adaptive Discretisations and Solvers, De Gruyter, 2017.
[70] X. Yuan, et al., Phase change cooling in data centers: a review, Energ. Buildings 236 (Apr. 2021) 110764, https://doi.org/10.1016/j.enbuild.2021.110764.
[71] W. Hua, L. Zhang, X. Zhang, Research on passive cooling of electronic chips based on PCM: a review, J. Mol. Liq. 340 (Oct. 2021) 117183, https://doi.org/10.1016/j.molliq.2021.117183.
[72] M. Bhatasana, Phase Change Materials for Die and Component Level Thermal Management, Faculty of Purdue University, West Lafayette, Indiana, 2024.
[73] A. Stupar, U. Drofenik, J.W. Kolar, Optimization of phase change material heat sinks for low duty cycle high peak load power supplies, IEEE Trans. Compon. Packag. Manuf. Technol. 2 (1) (Jan. 2012) 102–115, https://doi.org/10.1109/TCPMT.2011.2168957.